From the Department of Oncology and Pathology
Karolinska Institutet, Stockholm, Sweden

DEVELOPMENT OF RADIOMETAL-BASED LABELLING TECHNIQUES AND TRACERS FOR NON-INVASIVE MOLECULAR IMAGING

Emma Jussing

Karolinska Institutet

Stockholm 2022

Published by Karolinska Institutet.
Printed by Universitetsservice US-AB, 2022

ISBN 978-91-8016-484-9
Cover illustration: Graphical abstract that summarises the essential parts of the thesis.

Development of Radiometal-based Labelling Techniques and Tracers for Non-invasive Molecular Imaging

THESIS FOR DOCTORAL DEGREE (Ph.D.)

By

Emma Jussing

The thesis will be defended in public at Ulf von Euler lecture hall, J3:06, Karolinska University Hospital, Stockholm, Friday, March 25, 2022 at 9:00 am

Principal Supervisor:
Associate Professor Thuy Tran
Karolinska Institutet
Department of Oncology and Pathology and
Department of Clinical Neuroscience
Karolinska University Hospital
Department of Karolinska Radiopharmacy

Co-supervisor(s):
Ph.D. Erik Samén
Karolinska Institutet
Department of Oncology and Pathology
Karolinska University Hospital
Department of Karolinska Radiopharmacy

Professor Emeritus Sharon Stone-Elander
Karolinska Institutet
Department of Clinical Neuroscience

Professor Staffan Holmin
Karolinska Institutet
Department of Clinical Neuroscience
Karolinska University Hospital
Department of Neuroradiology

Opponent:
Associate Professor Danielle Vugts
Amsterdam UMC, VU University
Department of Radiology & Nuclear Medicine
Tracer Center Amsterdam

Examination Board:
Associate Professor Dirk Bender
Aarhus University
Aarhus University Hospital
Department for Nuclear Medicine and PET Center

Associate Professor Åsa Carlsson Tedgren
Karolinska Institutet
Department of Oncology and Pathology

Associate Professor Olof Eriksson
Uppsala University
Department of Medicinal Chemistry

To all my benefactors.

ABSTRACT

Metallic radionuclides, radiometals, have an important role in nuclear medicine. Their straightforward coordination radiochemistry allows for a large variety of applications. The similarities and differences between the radiometals can be utilised to expand the window of diagnostic imaging or transfer diagnostic methods from one imaging modality to another. Radiometals from the same or from different elements (both therapeutic and diagnostic) may be coordinated to similar probes, as a theranostic pair.

Radionuclide-based molecular imaging is a non-invasive *in vivo* imaging technique that quantifies the concentrations of radioactive probes in biological processes occurring at cellular and subcellular levels in living organisms. The two major diagnostic *in vivo* imaging techniques used are Single-Photon Emission Computed Tomography (SPECT) and Positron Emission Tomography (PET). In this thesis, radiometal production using a cyclotron solid target system and some fundamental aspects of radiometal labelling are explored, using two of the most common positron-emitting radiometals, gallium-68 (^{68}Ga) and zirconium-89 (^{89}Zr).

In **paper I** an albumin targeting Affibody molecule, ABY-028, was successfully developed, ^{68}Ga-labelled and *in vivo* evaluated using a small animal PET camera. We showed that the biodistribution was consistent with the binding of [^{68}Ga]Ga-ABY-028 to plasma albumin. Uptake patterns differed between tumours at different stages and of different phenotypes. Tracer uptake responses to permeability-altering therapeutics and during cerebral infarction could be observed. This novel radiotracer is a promising tool for *in vivo* molecular imaging of variations and alterations of vascular permeability and has the potential to function as a baseline control of the non-specific uptake of other albumin-binding domain (ABD)-based diagnostic or therapeutic agents. In **paper II** cells were ^{89}Zr-labelled, using two different metal complexes, with two distinctive labelling mechanisms, [^{89}Zr]Zr-(oxine)$_4$ and [^{89}Zr]Zr-DFO-NCS. Synthesis protocols were successfully optimised to yield high radiochemical conversions of both ^{89}Zr-complexes. Both radiotracers presented in this head-to-head study showed feasibility for universal radiolabellings of different cell types. The results suggested that [^{89}Zr]Zr-(oxine)$_4$ is most likely superior. In **papers III and IV** methods to meet the generally increasing demand for ^{68}Ga have been developed. In paper III a cyclotron-based solid target system was used for production and purification of the radionuclide. In paper IV a refinement method of the radionuclide's quality (regarding content of competing metal ions) was developed for clinical applicability for use in radiolabelling of DOTA-based radiopharmaceuticals, [^{68}Ga]Ga-DOTATOC and [^{68}Ga]Ga-FAPI-46. Compared to generator-derived ^{68}Ga, we successfully produced 10 times more product of both the radiopharmaceuticals using our solid target cyclotron-produced ^{68}Ga.

The strategies and approaches investigated and developed in this thesis have potential for translation to more exotic radiometals in the future, to potentially expanding the palette of chemical properties that can be used in radiolabelling, as well as the decay characteristics and time-windows for imaging. The methods and techniques for radiometal labelling explored in this thesis might also be translated to other specific tissue targeting molecules or cells.

SVENSK POPULÄRVETENSKAPLIG SAMMANFATTNING

Utveckling av radiometallbaserade märkningstekniker och spårämnen för icke-invasiv molekylär avbildning

Ett radiofarmakum är ett läkemedel som innehåller en radioaktiv komponent för medicinska ändamål. Läkemedlet består framför allt av två viktiga komponenter: En molekyl (spårämne) som bestämmer hur och var läkemedlet fördelar sig i kroppen och en radionuklid som avger den radioaktiva signalen eller den radioaktivt medicinska effekten. En radionuklid är en instabil atom som i sitt sönderfall, då den omvandlas till en stabilare form, avger strålning. Vid nuklearmedicinsk diagnostik registreras den radioaktiva signalen av speciellt anpassade kameror och omvandlas till bilder. Dess icke-invasiva natur betyder att inga fysiska ingrepp är nödvändiga (jämför t.ex. med vävnadsprov vid diagnostisk biopsi). Vid nuklearmedicinsk terapi avger istället läkemedlet lokal strålning till den vävnad som ska behandlas (t.ex. tumörer vid cancerbehandling).

I den här avhandlingen har vi arbetat med metalliska radionuklider, s.k. radiometaller. De kemiska egenskaperna hos radiometaller lämpar sig väl för tillverkning av radiofarmaka som innehåller spårämnen av större molekylstorlek (t.ex peptider eller proteiner). Dessa spårämnen har förmågan att binda till specifika mål i kroppen. Målen kan bestå av någonting som specifikt finns uttryckt på en viss typ av tumörer eller vid andra medicinska tillstånd. Målet för själva radiofarmakat behöver inte vara sjukdomsspecifikt vid diagnostik, men ska möjliggöra avbildning av fysiologiska förändringar i kroppen. Fysiologiska förändringar kan t.ex. bestå av förändrat blodflöde eller ämnesomsättning. Radiofarmaka, eller radionukliden ensam, kan också användas för att märka och följa administrerade antikroppar eller celler i kroppen. Terapier med antikroppar eller celler är både dyra och kan ge biverkningar. Vid utveckling av nya terapier av detta slag, och för att kunna avgöra vilka patienter som kan hjälpas av sådan behandling, är därför den radionuklidbaserade avbildningstekniken en viktig del i utvärderingsprocessen.

I det **första** ingående arbetet har ett albuminbindande spårämne, Affibodymolekylen ABY-028, utvecklats och radiomärkts med radiometallen gallium-68 (^{68}Ga). Dess bindning till albumin, ett protein rikligt förekommande i blodet, har sedan utvärderats i djurmodeller (gnagare). Vi kunde visa att distributionen av den radiomärkta [^{68}Ga]Ga-ABY-028 överensstämde med en bindning till albumin i blodet. Vi kunde också visa att [^{68}Ga]Ga-ABY-028 kan användas för att avbilda skillnader i genomsläpplighet av albumin mellan olika cancertyper och cancer i olika tillväxtfaser (stadier). Genomsläppligheten var förändringsbar med hjälp av kärlvidgande läkemedel. Förändringar av genomsläppligheten av albumin till hjärnan kunde också detekteras i en djurmodell av akut stroke. [^{68}Ga]Ga-ABY-028 kan även användas som ett kontrollspårämne vid utveckling och validering av nya målsökande spårämnen som är kombinerade med den albuminbindande delen av ABY-028. I det **andra** ingående arbetet har celler radiomärkts med radiometallen zirkonium-89 (^{89}Zr). Vi utvärderade och jämförde cellmärkningsmetoder med två olika metallkomplex, en där radionukliden fäster

på utsidan av cellen ([^{89}Zr]Zr-DFO-NCS) och en där radionukliden fångas inuti cellen ([^{89}Zr]Zr-(oxine)$_4$). Vi förbättrade tillverkningsmetoderna för båda ^{89}Zr-komplexen vad gäller effektivitet och stabilitet. Vi kunde också visa att dessa cellmärkningsmetoder kan användas universellt oberoende av celltyp. [^{89}Zr]Zr-(oxine)$_4$ var överlägsen [^{89}Zr]Zr-DFO-NCS i hållbarhetstid, alltså från tillverkningstillfället till att cellerna kunde radiomärkas. [^{89}Zr]Zr-(oxine)$_4$ hölls också kvar i cellerna under en längre tid, oberoende av celltyp, vilket är en stor fördel. Anledningen till att radiomärka celler är att vi ska kunna följa dem efter tillförsel i kroppen och med ^{89}Zr under en lång tid. I det **tredje** och **fjärde** arbetet har vi utvecklat en alternativ tillverkningsmetod med en partikelaccelerator (cyklotron) och reningsmetod (med en automatiserad modul) av ^{68}Ga, en radionuklid som har stor klinisk efterfrågan. Vi har sedan använt denna radionuklid för att tillverka kliniskt etablerade/lovande radiofarmaka som används vid cancerdiagnostik, [^{68}Ga]Ga-DOTATOC och [^{68}Ga]Ga-FAPI-46 – som utvärdering av dess användbarhet. Vi kunde med dessa sammankopplade arbeten visa på en överlägsen förbättring av mängden radiofarmaka (10 gånger mer) och deras hållbarhet när vi använde vårt cyklotronproducerade ^{68}Ga, jämfört med det ^{68}Ga som normalt sett utvinns från radionuklidgeneratorer.

De metoder som undersökts och utvecklats i denna avhandling har stor potential till att kunna överföras till andra mer exotiska radiometaller, vilka ännu inte blivit lika etablerade som ^{68}Ga och ^{89}Zr. Ett större urval av radiometaller, med olika kemiska egenskaper, kan bidra till en utveckling av och mer varierad radiofarmakatillverkning. Olikheter i radiometallernas sönderfall kan också bidra till att tiden för avbildning i den nukleärmedicinska kameran kan anpassas efter det diagnostiska behovet i högre grad. Vi kan med vår cyklotronutrustning tillverka en rad olika radiometaller, för vilka metoder är under utveckling. De metoder som vi använt för radiomärkning i denna avhandling har stor potential att kunna överföras till andra/nya målsökande spårämnen och/eller till andra typer av celler.

LIST OF SCIENTIFIC PAPERS

I. **Jussing, E.**; Lu, L.; Grafstrom, J.; Tegnebratt, T.; Arnberg, F.; Rosik, H.W.; Wennborg, A.; Holmin, S.; Feldwisch, J.; Stone-Elander, S. [^{68}Ga]ABY-028: an albumin-binding domain (ABD) protein-based imaging tracer for positron emission tomography (PET) studies of altered vascular permeability and predictions of albumin-drug conjugate transport. EJNMMI Res 2020, 10, 106, doi:10.1186/s13550-020-00694-2.

II. Friberger, I.; **Jussing, E.**; Han, J.; Goos, J.; Siikanen, J.; Kaipe, H.; Lambert, M.; Harris, R.A.; Samen, E.; Carlsten, M.; Holmin, S.; Tran, T.A. Optimisation of the Synthesis and Cell Labelling Conditions for [^{89}Zr]Zr-oxine and [^{89}Zr]Zr-DFO-NCS: a Direct In Vitro Comparison in Cell Types with Distinct Therapeutic Applications. Mol Imaging Biol 2021, doi:10.1007/s11307-021-01622-z.

III. Siikanen, J.; **Jussing, E.**; Milton, S.; Steiger, C.; Ulin, J.; Jonsson, C.; Samén, E.; Tran, T.A. Cyclotron-produced ^{68}Ga from enriched ^{68}Zn foils. Applied Radiation and Isotopes 2021, 109825, doi:10.1016/j.apradiso.2021.109825.

IV. **Jussing, E.**; Milton, S.; Samen, E.; Moein, M.M.; Bylund, L.; Axelsson, R.; Siikanen, J.; Tran, T.A. Clinically Applicable Cyclotron-Produced Gallium-68 Gives High-Yield Radiolabeling of DOTA-Based Tracers. Biomolecules 2021, 11, doi:10.3390/biom11081118.

Scientific papers not included in the thesis:

I. Jacobsson, H.; Larsson, P.; Jonsson, C.; **Jussing, E.**; Gryback, P. Normal uptake of ^{68}Ga-DOTA-TOC by the pancreas uncinate process mimicking malignancy at somatostatin receptor PET. Clin Nucl Med 2012, 37, 362-365, doi:10.1097/RLU.0b013e3182485110.

II. Arnberg, F.; Lundberg, J.; Olsson, A.; Samen, E.; Jaff, N.; **Jussing, E.**; Dahlen, U.; Nava, S.; Axelsson, R.; Ringden, O.; Kaipe, H.; Holmin, S. Intra-arterial Administration of Placenta-Derived Decidual Stromal Cells to the Superior Mesenteric Artery in the Rabbit: Distribution of Cells, Feasibility, and Safety. Cell Transplant 2016, 25, 401-410, doi:10.3727/096368915X688191.

III. Lundberg, J.; **Jussing, E.**; Liu, Z.; Meng, Q.; Rao, M.; Samen, E.; Grankvist, R.; Damberg, P.; Dodoo, E.; Maeurer, M.; Holmin, S. Safety of Intra-Arterial Injection With Tumor-Activated T Cells to the Rabbit Brain Evaluated by MRI and SPECT/CT. Cell Transplant 2017, 26, 283-292, doi:10.3727/096368916X693347.

IV. Sanchez-Crespo, A.; **Jussing, E.**; Bjorklund, A.C.; Pokrovskaja Tamm, K. Hallmarks in prostate cancer imaging with Ga68-PSMA-11-PET/CT with reference to detection limits and quantitative properties. EJNMMI Res 2018, 8, 27, doi:10.1186/s13550-018-0378-4.

V. Little, P.V.; Arnberg, F.; **Jussing, E.**; Lu, L.; Ingemann Jensen, A.; Mitsios, N.; Mulder, J.; Tran, T.A.; Holmin, S. The cellular basis of increased PET hypoxia tracer uptake in focal cerebral ischemia with comparison between [^{18}F]FMISO and [^{64}Cu]CuATSM. J Cereb Blood Flow Metab 2020, doi:10.1177/0271678X20923857.

VI. Dahl, K.; **Jussing, E.**; Bylund, L.; Moein, M.M.; Samen, E.; Tran, T. Fully automated production of the fibroblast activation protein radiotracer [^{18}F]FAPI-74. J Labelled Comp Radiopharm 2021, 64, 346-352, doi:10.1002/jlcr.3926.

CONTENTS

LIST OF ABBREVIATIONS

ABD	albumin-binding domain
ABY-025	Affibody molecule targeting HER2
ABY-028	Affibody molecule targeting albumin
^{225}Ac	actinium-225
A_m	molar activity
AMA	apparent molar activity
A_s	specific activity
BBB	blood-brain barrier
BC	breast cancer
^{11}C	carbon-11
cGRPP	current good radiopharmacy practice
^{55}Co	cobalt-55
^{62}Cu, ^{64}Cu	copper-62, -64
[^{64}Cu]Cu-ATSM	[^{64}Cu]Cu-diacetyl-bis[N(4)-methylthio-semicarbazone]
CT	computed tomography
3D	three-dimensional
DC	dendritic cells
DFO	deferoxamine
DNA	deoxyribonucleic acid
DOTA	1,4,7,10-tetraazacyclododecane-1,4,7,10-acetic acid
DOTATATE	DOTA-D-Phe1-Tyr3-octreotate
DOTATOC	DOTA-D-Phe1-Tyr3-octreotide
DTPA	diethylenetriaminepentaacetic acid
EC	electron capture
EDTA	ethylenediaminetetraacetic acid
ELISA	enzyme-linked immunosorbent assay
EOB	end of bombardment
^{18}F	fluorine-18

FAP	fibroblast activating protein
FAPI	FAP inhibitor
2-[^{18}F]FDG	2-deoxy-2-[^{18}F]fluoro-D-glucose
[^{18}F]FHBG	9-[4-[^{18}F]fluoro-3-(hydroxymethyl)butyl]guanine
^{66}Ga, ^{67}Ga, ^{68}Ga	gallium-66, gallium-67, gallium-68
$^{68}GaCl_3$	gallium-68 chloride
^{68}Ge	germanium-68
GMP	good manufacturing practice
HBED	N,N-bis(2-hydroxybenzyl)ethylenediamine-N,N-diacetic acid
HCl	hydrochloric acid
HEPES	4-(2-hydroxyethyl)-1-piperazineethanesulfonic acid
HER2,-3	human epidermal growth factor receptor 2, -3
HMPAO	hexamethylpropyleneamine oxime
HSAB	hard and soft acids and bases
HSV1-tk	herpes virus type 1 thymidine kinase
^{123}I	iodine-123
IAEA	international atomic energy agency
IMP	investigational medical product
IMPD	investigational medical product dossier
IgG	immunoglobulin G
IGF-1R	insulin-like growth factor 1 receptor
^{111}In	indium-111
^{177}Lu	lutetium-177
mAb	monoclonal antibody
mal-DOTA	1,4,7,10-tetraazacyclododecane-1,4,7-tris-acetic acid-10-maleimidoethylacetamide
^{52}Mn	manganese-52
^{99}Mo	molybdenum-99
MRI	magnetic resonance imaging
^{13}N	nitrogen-13
NaOAc	sodium acetate
NCS	isothiocyanate

NET	neuroendocrine tumour
NK	natural killer (cells)
NOTA	1,4,7-triazacyclononane-1,4,7-triacetic acid
^{15}O	oxygen-15
PC	prostate cancer
PD-L1	programmed death ligand 1
PET	positron emission tomography
PI	phosphor imaging
PSMA	prostate-specific membrane antigen
PSMA-11	PSMA-HBED
PSMA-617	PSMA-DOTA
RBC	red blood cells/erythrocytes
RCY	radiochemical yield
^{82}Rb	rubidium-82
RNP	radionuclidic purity
^{44}Sc	scandium-44
scFv	single-chain variable fragment
SPE	solid-phase extraction
SPECT	single-photon emission computed tomography
^{82}Sr	strontium-82
SSTR, -2	somatostatin receptor, -type 2
$t_{1/2}$	half-life
^{99m}Tc	technetium-99m
^{45}Ti	titanium-45
TiO_2	titanium oxide
WBC	white blood cells/leukocytes
^{86}Y, ^{89}Y, ^{90}Y	yttrium-86, -89, -90
^{67}Zn, ^{68}Zn	zinc-67, -68
^{89}Zr	zirconium-89

1 INTRODUCTION

Radionuclide-based molecular imaging is a non-invasive *in vivo* imaging technique that quantifies the concentrations of radioactive probes in biological processes occurring at cellular and subcellular levels in living organisms. The technique can be used to, for example, optimise drug therapy and image drug effects, to detect disease and to assess disease progression. The technique can be used to monitor the same individual over time [1]. Molecular imaging provides information that is beyond what is possible to detect from purely anatomic imaging (such as x-ray or computed tomography (CT)) – it traces altered chemical processes and/or cellular alterations not yet visible to the eye [2,3].

Because the radionuclide-based imaging technique tracks radionuclide-labelled molecules, radiopharmaceuticals/radiotracers, it is a true molecular imaging technique. In general, a radiopharmaceutical consists of two important components: the molecule that decides the pharmacokinetic and pharmacodynamic fate and the radionuclide responsible for the detectable signal [4].

The interest in molecular imaging techniques is rapidly increasing, which means the research on and the development of new radiopharmaceuticals need to keep a similar pace [5]. An increasing demand for more specific targeting tracers is driven by research on the relationships between cell surface expressing proteins, disease progression and potential diagnostic strategies, especially in cancers [6].

Specific cancer-targeting therapeutics often involve larger molecules (e.g. polypeptides or proteins) or cells. These are often effective but can also be expensive and there are always potential risks from side effects. Molecular imaging can successfully stratify patients for these therapies, but careful considerations of the radionuclides and labelling methods are necessary. Metallic radionuclides, so-called radiometals, possess suitable characteristics for labelling these types of therapeutics, or molecules/tracers engineered for binding to the same target in tissue. Some fundamental aspects of radiometal labelling are explored in this thesis. In paper I one highly specific targeting polypeptide is radiolabelled using generator-derived gallium-68 (^{68}Ga), a relatively short-lived radiometal, and evaluated. In paper II cells are labelled, using two different techniques, with the cyclotron-produced and long-lived radiometal zirconium-89 (^{89}Zr), a more suitable choice for the *in vivo* tracking of cells over longer periods of time [7]. In papers III and IV methods to meet the generally increasing demand for ^{68}Ga are investigated, by developing a cyclotron-based solid target production of the radionuclide (paper III) and refining its quality and validating its implementation in the radiolabelling of clinically relevant radiopharmaceuticals (paper IV).

1.1 CANCER

Cancer is the leading cause of death in economically developed countries. In the latest update of the Global Burden of Disease Study [8] an incidence of an estimated 23.6 million new cancer

cases were diagnosed in 2019 globally. This trend of constantly increased cancers is now most pronounced in the low-middle economically developed countries.

Normally, cells of the body are well organised in cycles of growth and division. When damaged or old, they die and new cells take their place. Normal cells don't invade beyond other types of cells, e.g. normal liver cells would not suddenly decide to start up a new liver organ in the area of the lung. In cancer cells this organisation is disrupted.

Cancer is a collective name for diseases with the common characteristic of uncontrolled cell division, leading to abnormal growth and invasion of distant tissues. The disrupted organisation, contrary to the normal cell cycle homeostasis, is caused by inherited or acquired genetic mutations. The extent and patterns of mutations are unique for every cancer, but two fundamental traits must be acquired early in the cancerous process – the ability to proliferate without normal controlled stimuli and the ability to avoid antiproliferative signals [9].

Cancers are not solely growths of individual proliferating cancer cells, but rather are much more complex compositions of these cells in their microenvironment. Hallmarks of cancers include sustaining proliferative signalling, evading growth suppressors, enabling replicative immortality, avoiding immune destruction, tumour promoting inflammation, activating invasion and metastasis, inducing angiogenesis, genome instability and mutation, resisting cell death and deregulation of cellular energetics [10].

Although every cancer is unique, some distinguishing characteristics are more common, but not entirely exclusive, among cancers originating from specific tissues. Examples of these characteristics, biomarkers, are elevated densities of human epidermal growth factor receptor type 2 (HER2) in many breast cancers (BC) [11], prostate specific membrane antigen (PSMA) receptors in prostate cancers (PC) [12] and somatostatin receptors (SSTR) of various subtypes in neuroendocrine tumours (NET) [13]. These morphological changes are the results of cancerous mutations promoting proliferation and growth. These differences compared to normal cells present opportunities for more specific targeted therapies, sparing surrounding healthy tissues. HER2 positive (HER2+) cancers have been treated successfully for many years with the monoclonal antibody (mAb) trastuzumab [14] and SSTR positive (SSTR+) cancers with octreotide [13]. To select patients more likely to respond to these targeted therapies it is important to investigate the density and distribution of receptors in each individual cancer patient, especially when metastasis is suspected or when the expression of biomarkers is found to be typically heterogeneous. These biomarkers can potentially also be utilised for targeted radiotherapeutics, as with the proposed beta-emitting (β-) lutetium-177 (^{177}Lu) radiolabelled [^{177}Lu]Lu-PSMA-617 in the treatment of PC [15] or [^{177}Lu]Lu-DOTATATE/Luthathera (SSTR agonist) in the treatment of NET [16].

Radionuclide-based molecular imaging to stratify patients for targeted cancer treatments is well accepted in NET using [^{68}Ga]Ga-DOTATOC [17] and in PC using [^{68}Ga]Ga-PSMA-11 [18]. Diagnostic radiopharmaceuticals imaging HER2+ BC are currently being investigated [11], of which [^{68}Ga]Ga-ABY-025 is a promising candidate [19].

Overall, the opportunities to investigate potential target specific therapeutic and diagnostic agents ranging from small molecules to polypeptides to cells in the fight against cancer are nearly endless. Radionuclide-based molecular imaging of biochemical processes or cell migration offers *in vivo* visualisation and quantification capabilities that are unique compared to anatomic imaging or traditional biochemical sampling. Radiometals possess characteristics suitable for labelling these targeting agents, which makes research in this area timely and potentially very valuable.

1.2 THE IMAGING SYSTEMS

The two major diagnostic *in vivo* radionuclide-based molecular imaging techniques used are Single-Photon Emission Computed Tomography (SPECT) and Positron Emission Tomography (PET) [20,21]. These imaging techniques are briefly described below.

1.2.1 Single-Photon Emission Computed Tomography

In SPECT the single gamma (γ) photons emitted during the radioactive decay of the administered radionuclide are detected by scintillator crystals that are rotated around the subject, collimated, and spatially localised. See Figure 1. The different radionuclides emit single photons of different energies, which are distinguished by the SPECT/gamma camera [2]. This imaging technique was not utilised in the work of this thesis, but it has played a large role in routine clinical nuclear medicine imaging. Much of its success lies in the widespread access to the easily handled generator-derived single-photon emitting radionuclide technetium-99m (^{99m}Tc) and the wide range of its one-step kit-based labelling procedures available. These radiolabelled compounds are widely used clinically for e.g. perfusion and skeletal imaging and less often for the more specific targeting diagnostic approaches such as those used with PET radiopharmaceuticals [22].

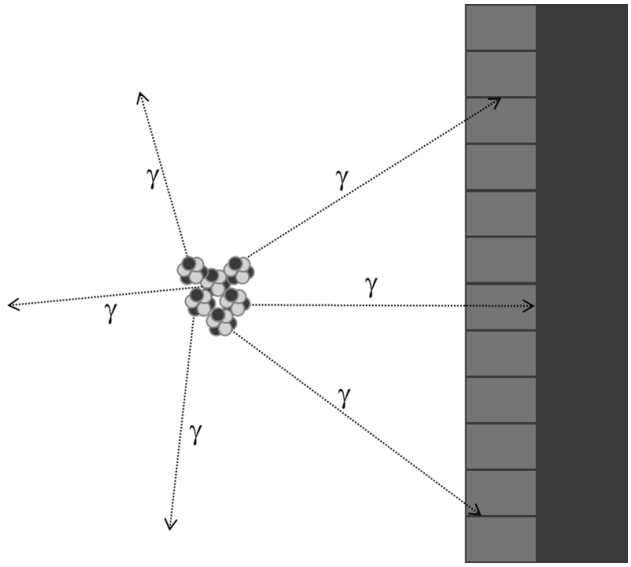

Figure 1. Schematic illustration of SPECT.

1.2.2 Positron Emission Tomography

In PET large numbers of scintillator crystals with photomultiplier tubes are arranged around the subject to detect the coincident 511 keV photons emitted during the decay of the administered radionuclide. In the decay process a positron (β^+) is emitted from the nucleus. See Figure 2.

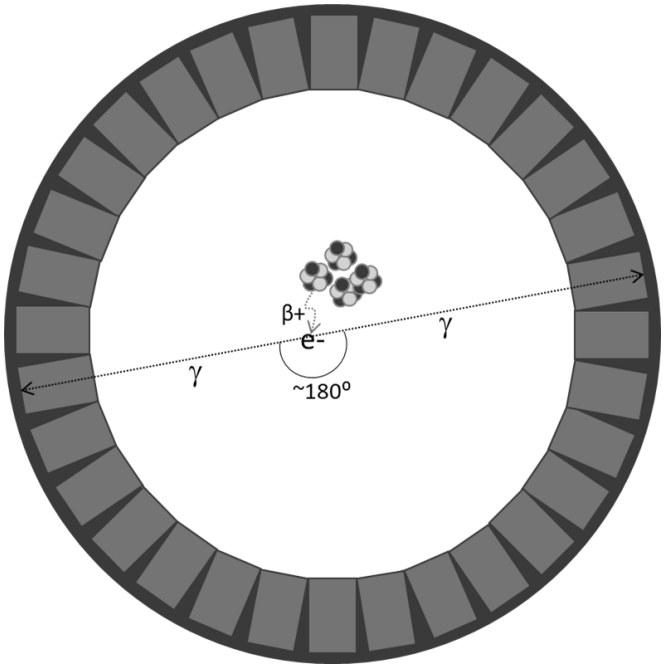

Figure 2. Schematic illustration of PET.

The positron travels up to a few millimetres before colliding with an electron (e^-) and is annihilated. Two gamma photons are then emitted in opposite directions and are co-registered by two detectors in the camera (coincidence detection). The distance the positron travels before annihilation depends on both the energy of the positron and the density of the tissue. A high energy positron will travel a longer distance before annihilation and will thereby reduce the spatial resolution [23]. See Figure 3. In clinical use, PET is more sensitive and has better resolution and quantifying capability than SPECT [2,24]. The differences in spatial resolution for the different radionuclides may not critically affect the image quality in the large subjects in clinical studies, but in preclinical studies with small animals resolution losses may determine whether or not the PET radionuclide can be used for imaging [25].

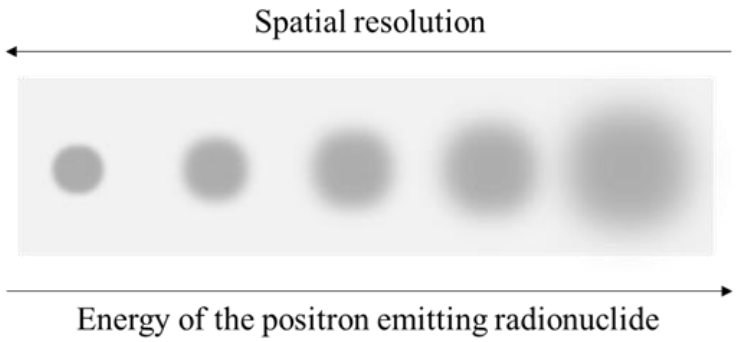

Figure 3. Graphic illustration of the relationship between the energy of the positron-emitting radionuclide and the PET image spatial resolution.

1.2.3 Multimodality imaging

Combining two or more imaging modalities in a single investigation can increase as well as improve the information obtained. Both PET and SPECT collect molecular information by tracking the gamma photons emitted in the decay of radioactive molecules but lack anatomical information. The combination of PET with CT is standard in oncological imaging today, with anatomical guidance by CT facilitating and improving the diagnostic interpretation of the PET images [26]. Similar improvements have been gained by combining SPECT with CT. Multimodality imaging of PET or SPECT together with magnetic resonance imaging (MRI) is also used clinically, although not to the same extent as with CT. The PET/MRI or SPECT/MRI multimodality imaging combinations are mostly used when the diagnostic questions concern soft tissues, as CT gives very little soft tissue information [27]. MRI is currently primarily used for the same purpose, for anatomical guidance, but has additional potential utilisations. MRI is a molecular imaging technique that quantifies magnetic/polarised molecules *in vivo*, e.g. the water molecules that are rich in soft tissues. This capability may be exploited for developing multimodality probes for PET/MRI or SPECT/MRI to enable the simultaneous imaging of multiple biochemical processes *in vivo* [28].

1.2.4 Phosphor imaging

In phosphor imaging (PI) a plate consisting of a thin layer of phosphor crystals is exposed to radioactivity, causing ions in the crystals to oxidise. The electrons released from the oxidation of ions are stored in the phosphor crystal layer in proportion to the radioactivity exposed to the plate. After exposure the plate is scanned with a phosphor imager where a laser releases the electrons, reducing the ions back to their original state. In this reduction light is released and detected, creating an image of areas dense in radioactivity [29,30].

Any radioactive material may be scanned using a phosphor imager to visualise the distribution of radioactivity. The technique is often used in combination with preclinical small animal imaging for *ex vivo* confirmation of radiotracer/radiopharmaceutical uptake in tissue. This confirmation is especially important for small regions that require higher spatial resolution or for regions surrounded by tissues with large radioactivity uptake causing a spill over effect in the images [29]. See example in Figure 4. PI was used in paper I of this thesis to estimate the equilibrium binding constant (Kd) of [^{68}Ga]Ga-ABY-028 and for *ex vivo* confirmation of uptake in rat brain.

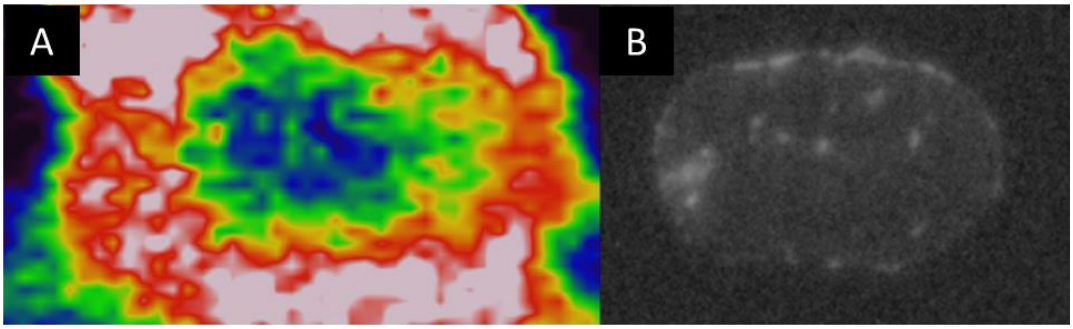

Figure 4. Imaging of rat brain after injection of ^{68}Ga-labelled radiotracer using two different imaging modalities, A = PET, in vivo, B = PI, section ex vivo. Images from author's own unpublished data.

1.3 THE RADIONUCLIDE

The radionuclide part of a radiopharmaceutical imparts its mechanism of action through its decay [31]. A radionuclide's decay chain may consist of a single emission route or a mixture of radiation generating emission routes [32].

When the radiopharmaceutical is used as a therapeutic agent (i.e. radionuclide therapy) the radiation consists primarily of particle emissions, as alpha or beta particles or Auger electrons [33]. When the radiopharmaceutical is used in diagnostic non-invasive molecular imaging, gamma photons are released in the radionuclide's decay chain. The energy of the photons needs to be high enough to penetrate the object, but low enough and suitable for collimation and detection by the imaging equipment.[31]

1.3.1 Common *in vivo* imaging radionuclides

The radionuclides most commonly used in SPECT are the halogen iodine-123 (^{123}I) and the metals ^{99m}Tc and indium-111 (^{111}In). The most commonly used PET radionuclides are the non-metals fluorine-18 (^{18}F), carbon-11 (^{11}C), nitrogen-13 (^{13}N), oxygen-15 (^{15}O) and the metal ^{68}Ga. See Table 1.

Table 1. The most commonly used radionuclides in SPECT and PET. The photons from PET radionuclides detected in PET imaging all have an energy of 511 keV.

SPECT	$t_{1/2}$	Energy (keV)
^{111}In	2.8 days	173/247
^{123}I	0.6 days	159
^{99m}Tc	6.0 hours	140

PET	$t_{1/2}$
^{18}F	109.8 min
^{68}Ga	67.8 min
^{11}C	20.4 min
^{13}N	10.0 min
^{15}O	2.0 min

1.3.2 Radiometals

Radiometals have distinctive chemical properties whose similarities and differences can be exploited to label different tracer molecules and to adjust the time windows during which processes can be imaged with nuclear medicine techniques. Among the radiometals suitable for diagnostic imaging (e.g. positron-emitting ^{64}Cu, ^{68}Ga, ^{89}Zr and gamma-emitting ^{111}In and ^{99m}Tc), the differences in their decay routes and half-lives decide which imaging technique to use (i.e. PET or SPECT) and the time windows during which a given biochemical process can be followed *in vivo*. Optimal conditions are achieved in diagnostic molecular imaging when the half-life of the radionuclide is just long enough to follow the investigated biochemical process, but short enough to avoid unnecessary radiation burden [34].

In this thesis the radiometals ^{68}Ga and ^{89}Zr were explored. These radiometals were chosen because their positron-emitting capabilities allowed PET imaging and because their different half-lives are suitable for the respective applications.

1.3.2.1 Gallium-68 (^{68}Ga)

^{68}Ga has a half-life of 67.7 minutes and decays 89% by positron emission and 11% by electron capture (EC). The radionuclide has a relatively high positron energy (mean β+ energy 836.0 keV, maximum β+ energy 1899.1 keV) [35]. In aqueous solutions gallium is found in the Ga(III) form and is not further reduced or oxidised in physiological conditions. According to the principle hard and soft (Lewis) acids and bases (HSAB) classification, gallium is a hard acid and coordinates most preferably with hard bases, such as O and N, often forming a six-coordinate octahedral geometry with the chelating ligand. In the pH range that is relevant for radiolabelling biomolecules (pH 3-7) gallium forms an insoluble hydroxide ($Ga(OH)_3$), the colloidal form of the metal. To circumvent colloidal formation, weak acids (e.g. acetate, citrate or oxalate) are often used in ^{68}Ga-labelling to create coordinations with the metal that are strong enough for this purpose, but weak enough to not interfere with the metal's subsequent coordination in the radiopharmaceutical complex [3,36,37].

^{68}Ga has been used in nuclear medicine for many years, even before ^{99m}Tc radiopharmaceuticals and 2-deoxy-2-[^{18}F]fluoro-D-glucose (2-[^{18}F]FDG) became standards in the clinical setting. As the handling of the first germanium-68(^{68}Ge)/^{68}Ga generators (described in more detail in section 1.4.1) was at that time cumbersome and not suitable for easy radiolabelling, the radionuclide was set aside in favour of others, such as ^{99m}Tc and ^{18}F [38]. With the introduction of more easily-handled generators [39] the interest for ^{68}Ga increased again, especially since the development of chemistry suitable for the target specific ^{68}Ga-labelled radiopharmaceuticals. Today ^{68}Ga is involved in the most publications and clinical trials, compared to all positron-emitting radiometals [40]. Only a few years ago ^{68}Ga would not have made the list of radionuclides "commonly" used in PET, which indicates its rapid increase in popularity.

1.3.2.2 Zirconium-89 (^{89}Zr)

^{89}Zr has a half-life of 78.4 hours and decays 23% by positron emission and 77% by EC. The radionuclide has a relatively low positron energy (mean β+ energy 395.0 keV), which results in a high image spatial resolution (compared to ^{68}Ga) [41]. The large proportion of the EC decay route to ^{89m}Y results in a 909.9 keV gamma decay to stable ^{89}Y, which must be considered carefully in patient dosimetry calculations and in effective doses absorbed by personnel [42]. Zirconium has several oxidation states, but is found preferably in its Zr(IV) form in solution. According to the HSAB classification zirconium is an extremely hard acid and coordinates most preferably with hard bases such as O, but also with N, and has the ability to form an eight-coordinate geometry with the chelating ligand [43].

Due to the radionuclide's suitable chemical properties, 78.4 hour half-life and low energy photons yielding PET images of high spatial resolution, ^{89}Zr has become widely used for imaging vectors with extended biological distribution patterns, such as antibodies [44]. In clinical studies ^{89}Zr is of emerging interest for tracking cells using PET imaging for studies of distribution patterns and homing related to cell therapies [45]. For example, a clinical study imaging autologous leukocytes and their capability to penetrate the brain was initiated, using [^{89}Zr]Zr-(oxine)$_4$ for *in vitro* cell labelling [46].

1.3.2.3 Other positron-emitting radionuclides

Another prominent PET radiometal is copper-64 (^{64}Cu), with a half-life of 12.7 hours, making it a suitable candidate for labelling molecules with intermediate *in vivo* distributions. The low β+ energy of ^{64}Cu will give high spatial resolution and there is also an interest in the additional Auger electrons emitted in its decay, which suggest this radionuclide as a true theranostic [47]. Copper is redox-inert in physiological conditions, which is a problem for chelations to pharmaceutical ligands and can potentially cause decomplexation *in vivo*. However, the most studied ^{64}Cu-complex, [^{64}Cu]Cu-ATSM, successfully utilises this property for imaging hypoxic tumours [48].

The short-lived ($t_{1/2}$ 1.3 minutes) radiometal rubidium-82 (^{82}Rb) has been used in cardiac perfusion studies for many years [49], but is too short-lived for more complex radiopharmaceutical productions. Other radiometals, e.g. cobalt-55 (^{55}Co), copper-62 (^{62}Cu), manganese-52 (^{52}Mn), scandium-44 (^{44}Sc), titanium-45 (^{45}Ti), and yttrium-86 (^{86}Y) are promising, which are referred to as "exotic" radiometals later in the concluding remarks and future perspectives section of this thesis.

1.4 GENERATOR-DERIVED RADIONUCLIDES

One of the central pillars in nuclear medicine is the access to suitable radionuclides. Radionuclide generators have been especially important for hospitals without an on-site cyclotron, but also for increasing the radionuclides available at hospitals with an on-site cyclotron. In a radionuclide generator system, the (often more long-lived) parent radionuclide

is loaded on a column matrix where, in its decay route, a daughter radionuclide is produced. The daughter radionuclide is then separated from its parent for use in nuclear medicine diagnostic or therapeutic applications. The most commonly used radionuclide in nuclear medicine worldwide, ^{99m}Tc, is derived from molybdenum-99 (^{99}Mo) generators [50]. ^{99m}Tc is widely used in SPECT and, to make this convenient generator technique accessible to PET, a variety of possible parent/daughter pairs are suggested [51]. The currently most commonly used of these are the strontium-82 (^{82}Sr)/^{82}Rb [49] and the ^{68}Ge/^{68}Ga generators [52]. With a half-life of 67.7 minutes ^{68}Ga is well suited for labelling peptides with fast to intermediate pharmacokinetics. The ^{68}Ge/^{68}Ga generator was used in paper I.

1.4.1 The ^{68}Ge/^{68}Ga generator

The first ^{68}Ge/^{68}Ga generators were cumbersome, suffered from unacceptable levels of ^{68}Ge breakthrough (half-life 271 days) or gave ^{68}Ga-complexes that had to be modified before radiolabelling could be performed. The ^{68}Ge/^{68}Ga generators of today are much convenient [52]. Thanks to the development of generators based on ^{68}Ge adsorbed on a titanium oxide (TiO_2) solid phase column with ionic ^{68}Ga eluted in weak hydrochloric acid (0.1 N HCl), radiolabelling chemistry became manageable and ^{68}Ge breakthrough was minimised [51,52]. See Figure 5.

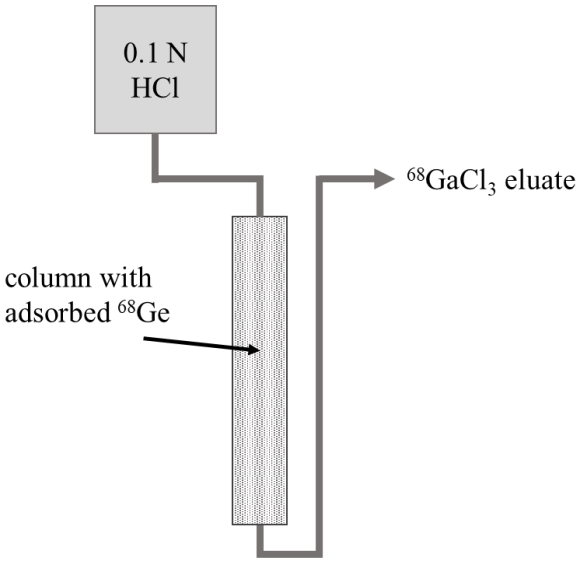

Figure 5. Schematic illustration of a modern ^{68}Ge/^{68}Ga generator.

1.5 CYCLOTRON PRODUCTION OF RADIONUCLIDES

1.5.1 The cyclotron

The charged particles accelerated in a so-called medical cyclotron situated in hospitals today are typically negative ions made from either hydrogen or deuterium gas. The charged particles are extracted from the ion source, placed in the centre of the cyclotron, by a radio frequency (RF) system, and enter inside one of the two metal electrodes. The two D-shaped metal electrodes are called “dees”, referring historically to their original shape. The dees are placed

between the poles of an electromagnet, which generates a static magnetic field. The magnetic field (B) bends the charged (q) particles in a circular path at a velocity (v) with radius (r). The cyclotron angular frequency $\omega=qB/m$ can be derived from the fact that the magnetic Lorentz force ($F_m=qvB$) will be equal to the centripetal force ($F_c=mv^2/r$). Since ω is not dependent on the radial position the revolution time, $T=2\pi m/qB$, will be constant. By feeding an alternating voltage, with the same frequency as the cyclotron frequency, to the dees it is therefore possible to accelerate the particles in the electric field created between the dees over and over again since the phase of the alternating voltage will be the same at each passage. Every time the particle passes the gap between the dees their kinetic energy and their radial position increases. This results in a spiral trajectory from the ion source out to the periphery of the magnet.

When the charged particles reach the periphery of the magnet, they pass a foil that strips off electrons from the particles, changing their charge from negative to positive. Therefore, the magnetic bending force applied to the charged particles will switch directions 180 degrees and now instead bend them out from the cyclotron magnet. In this way the beam can be extracted from the cyclotron and directed to different target stations. The target can be a gas, a liquid, a suspension, or a solid material. A useful nuclear reaction for medical cyclotrons is the p,n-reaction, in which the target material is bombarded with protons and a neutron is removed. A new unstable proton rich radionuclide often useful for PET is created [53]. See Figure 6. The most commonly used non-metallic PET radionuclides (^{18}F, ^{11}C, ^{15}O and ^{13}N) are produced by irradiating gas or liquid targets [54].

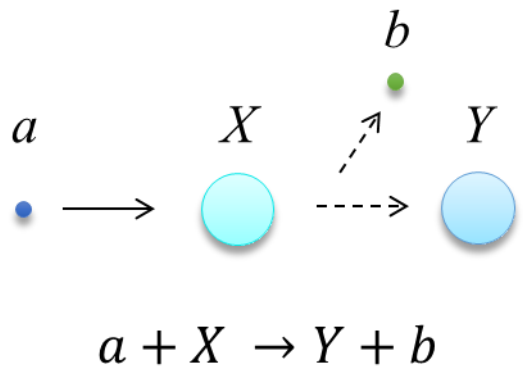

Figure 6. Particle bombardment of target material in the cyclotron (a = accelerated particle, X = target atom, Y = new unstable element, and b = reaction product)

1.5.2 Cyclotron production of radiometals

Many radiometals can be obtained by irradiating solid or liquid targets using medical cyclotrons. A liquid target has the advantage that the radiometal will already be in solution at the end of bombardment (EOB), facilitating the transfer to the subsequent separation and radiopharmaceutical production unit. A solid target has a main advantage of giving higher yields, due to the much higher concentration of the target material [55]. See Table 2.

Table 2. A brief comparison of advantages and disadvantages of the liquid and solid target systems, exemplified with ^{68}Ga.

^{68}Ga liquid target	^{68}Ga solid target
Low/medium yields ($\leq$ 2.5 GBq $^{68}GaCl_3$)	High yields (up to 130 GBq $^{68}GaCl_3$)
^{68}Ga already in solution after bombardment, ready for separation from its parent ^{68}Zn and other unwanted metal contaminants.	The solid target must normally be dissolved after bombardment, before ^{68}Ga separation from its parent ^{68}Zn and other unwanted metal contaminants.
Co-production of ^{13}N and risk of ^{66}Ga and ^{67}Ga co-production.	Risk of ^{66}Ga and ^{67}Ga co-production.
Excellent when little/medium demand for ^{68}Ga-labelled molecules. Cyclotron is needed.	Excellent when high demand for ^{68}Ga-labelled molecules. Cyclotron and additional equipment are needed.

1.5.2.1 Liquid target production of radiometals

The simplicity in loading and unloading a solution to and from a target body makes the liquid target radiometal production approach attractive. There are, however, some parameters that require consideration. First of all, the target is loaded in a solution. This means there can be limitations due to solubility, which is also the limiting factor for production output. Challenges due to high pressures in the target body have also been reported. These are interpreted to be caused by rapid gas evolution due to the radiolysis of water and depend on the metal and salt chosen (e.g. M_xNO_x or M_xCl_x) [56,57].

1.5.2.2 Solid target production of radiometals

Using solid targets enables a maximum density of the target material compared to liquid targets, which results in a much higher radioactivity output. See Table 3 for examples of radiometals possible to produce using the solid target system and the cyclotron at the Karolinska University Hospital (Comecer EDS/PTS and GE Healthcare, PETtrace 800). The metal to be irradiated can be prepared in different ways : electroplated to a metal disc [58-60], pressed into a coin [61], fused into a coin [62], sputtered to a backing material [63] or shaped as a foil [64]. The solid material is then placed in a holder (shuttle) and transferred to the target body for subsequent irradiation. To fully utilise the high activity output from a solid target system, it is essential to automate this transfer to minimise dose exposure [55]. At the Karolinska University Hospital a pneumatic transfer system is used for transferring the shuttle back and forth between the target body and the dissolution station.

Table 3. Examples of radiometals that can possibly be produced using the solid target system at the Karolinska University Hospital.

PET Radiometal	Half-life	Cyclotron production route
^{68}Ga	67.7 min	^{68}Zn(p,n)^{68}Ga
^{45}Ti	3.1 hours	^{45}Sc(p,n)^{45}Ti
^{64}Cu	12.7 hours	^{64}Ni(p,n)^{64}Cu
^{55}Co	17.5 hours	^{58}Ni(p,α)^{55}Co or ^{54}Fe(d,n)^{55}Co
^{89}Zr	3.3 days	^{89}Y(p,n)^{89}Zr or ^{89}Y(d,2n)^{89}Zr

1.5.2.3 Common production requirements

Solid and liquid target systems differ in many aspects. However, the end product and goal are essentially the same – the production of a radionuclidic- and chemically pure radiometal.

The radionuclidic purity (RNP) (see definition in Equation 1) is dependent on the isotopic purity of the target material, but may also depend on the proton energy with which the target is irradiated. For example, in an International Atomic Energy Agency (IAEA) summary regarding the cross-section cyclotron production dependency of ^{68}Ga [55], it is described that a proton energy above 12.2 MeV produces long-lived ^{67}Ga through the ^{68}Zn(p,2n)^{67}Ga reaction. See Figure 7. Even when an energy lower than 12.2 MeV is chosen ^{67}Ga will still be produced through the ^{67}Zn(p,n)^{67}Ga reaction, due to the ^{67}Zn impurity in the enriched ^{68}Zn. For the production of ^{89}Zr, impurities of other isotopes of yttrium are not problematic, since the natural abundance of ^{89}Y is 100%. However, the proton energy for the ^{89}Y(p,n)^{89}Zr reaction does have to be considered, since ^{89}Y(p,2n)^{88}Zr will occur at energies above 13.1 MeV [64,65].

$$RNP_a = A_a/(A_a+A_b+A_c+A_d\ldots)$$

Equation 1. The definition of radionuclidic purity (RNP), where RNP_a = the radionuclidic purity of radioisotope a, A_a = radioactivity associated with radioisotope a, $A_b+A_c+A_d\ldots$ = total radioactivity from all radioisotopes co-produced with a.

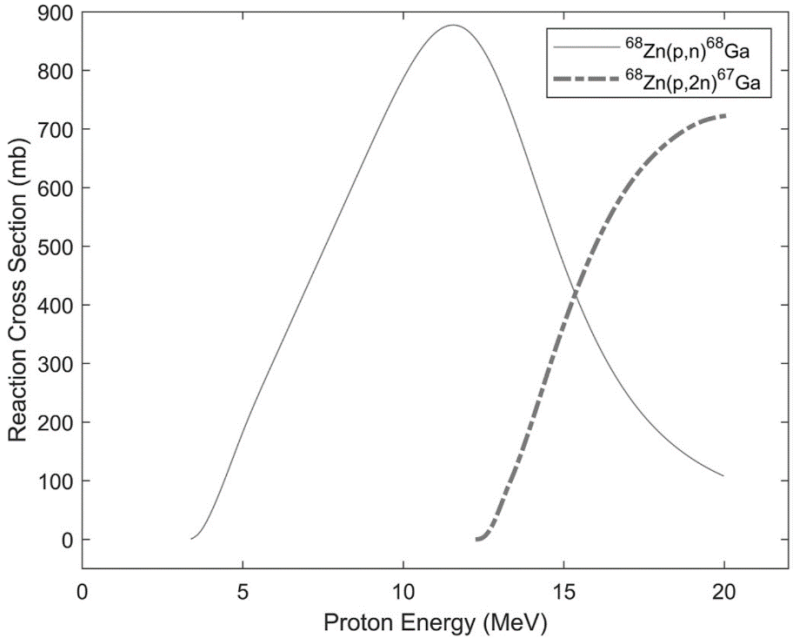

Figure 7. Recommended cross-sections for the ^{68}Zn(p,n)^{68}Ga and ^{68}Zn(p,2n)^{67}Ga proton energy dependent reactions [66].

To obtain a radiometal solution that is useful for radiolabelling it is crucial to reduce the competing radioactive as well as non-radioactive metal ions. Competing metal ions are those that will challenge the radionuclide for the intended labelling site on the radiopharmaceutical. These competing metal ions often originate from the irradiated target material, from poorly cleaned tubes or from chemicals used in the production/separation process. To reduce these contaminants, ultra pure chemicals and separation methods are used. Historically, different liquid-liquid extraction separations were used [64]. Today ion exchange solid-phase separation methods that separate ions of different elements by charges are most often used [58,64,67,68], which greatly simplifies automation.

1.5.3 Apparent molar activity

Molar activity (A_m) and specific activity (A_s) are values calculated from the amount of the radionuclide and all other isotopes from the same element present in the labelled radiopharmaceutical compound. A_m and A_s are values often used in the radiochemistry of, for example, ^{18}F or ^{11}C, because they will tell us how many non-radioactive atoms that the radioactive atoms have to compete with in the radiolabelling [69]. In radiometal chemistry, there is a need to also consider other metal ions that are also capable of binding to the radiopharmaceutical. A better value to use in radiometal chemistry is therefore the apparent molar activity (AMA), a value that is calculated through experimental titrations (which were performed in paper III and IV). This value tells us something about the amount of competing metal ions present and also about the possibility for the radiometal ion to label a radiopharmaceutical or chelator [55]. The chelator is described in section 1.6.3.

1.6 RADIOLABELLING STRATEGIES WITH RADIOMETALS

There are a number of parameters to consider regarding the choice of radionuclide when planning a radiolabelling strategy for a certain molecule. Availability of the radionuclide is obviously of great importance, as are its physical, radiochemical and/or radiopharmacological characteristics [4].

The most widely used PET radionuclides are the non-metals ^{18}F and ^{11}C, with half-lives of 109.8 and 20.3 minutes respectively. These radionuclides have the ability to form covalent bounds to carbon atoms, which means they can be incorporated into molecules (e.g. endogenous molecules or pharmaceuticals) without, or by very little, changing the molecules' structure. Small molecules require this type of radiolabelling [34]. A well-known example is the glucose analogue 2-[^{18}F]FDG.

Radiolabelling strategies with ^{18}F and ^{11}C most often require high temperatures and harsh chemical environments that are not suitable for larger biomolecules (e.g. polypeptides, single-chain variable fragments (scFv) or antibodies). To avoid degradation of larger molecules in the radiolabelling process, using a radiometal together with a chelator coupled to the molecule is often a favourable strategy [34,70]. See Figure 8.

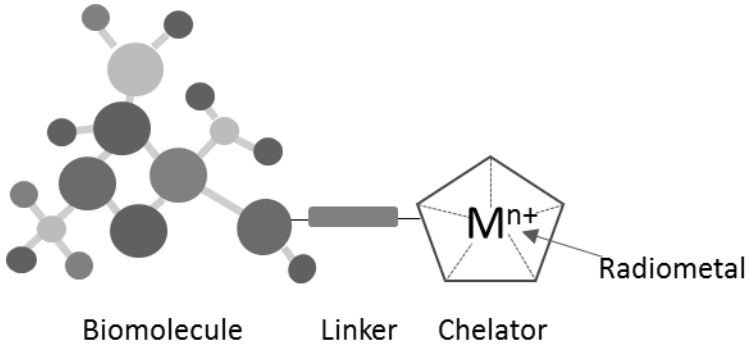

Figure 8. Illustration of a typical radiometal labelled tracer containing the targeting biomolecule, a linker, a chelator and the complexed radiometal.

As mentioned previously, radiometals have distinctive chemical properties whose similarities and differences can be exploited to label potential tracer molecules. Some factors that need to be considered in radiometal radiolabelling are discussed briefly below.

1.6.1 Reaction solution

The pre-formulation solution of the radiometal must be suited for the intended radiolabelling procedure. When introduced to the reaction vial containing the precursor/ligand and buffer solution, the radiometal may be in its ionic form (e.g. [^{68}Ga]$GaCl_3$, [^{89}Zr]$ZrCl_4$) or complexed (e.g. [^{89}Zr]Zr-$(oxalate)_4$). When choosing the ionic formulation, it is important to consider the risk of colloid formation, while it is crucial for complex formulations that the stability constant is not higher than for the complex/chelation in the subsequent radiolabelling, the

radiopharmaceutical production [3,71]. Re-formulation of the radionuclide is sometimes also used to decrease the reaction volume (i.e. increase the concentration and thereby the reaction speed), to gain better control of the reaction solution (i.e. pH-value), to minimise manual adjustments (i.e. saving time, less dose exposure to the operator) [71-73].

Typical buffers used in radiometal labelling commonly consist of sodium acetate (NaOAc) or 4-(2-hydroxyethyl)-1-piperazineethanesulfonic acid (HEPES). Depending on the choice of radiometal and chelating ligand, different pH values and temperatures are used [34,74]. Additions of ethanol (EtOH) and ascorbic acid are sometimes also included in the reaction solution. EtOH is used to break the hydration shell around the radiometal cation to facilitate the radiometal-ligand formation and/or to prevent radiolysis [75]. Ascorbic acid is used as a buffering agent and/or to prevent radiolysis [76,77]. However, the use of ascorbic acid when labelling with ^{89}Zr and ^{64}Cu should be carefully considered, due to the possibility of reducing the radiometals and causing demetallation of the radiopharmaceutical complex [78,79].

1.6.2 Post-labelling purification and product formulation

Purification of the radiolabelled product is needed when the radiometal-ligand complexation reaction is not complete or fully satisfying, and/or it contains high degree of impurities. Free radiometal ions will likely distribute *in vivo* differently than the radiopharmaceutical and will cause elevated image background uptake (see Figure 9). Smaller molecules or peptides are often purified using reversed solid-phase extraction (SPE) columns, such as C18 SepPak or Oasis HLB [80,81], while size exclusion columns, for example gel filtration columns, are used to purify radiometal-complexes with larger molecules (e.g. antibodies). Sometimes excess chelator is added before the post-purification step to more effectively remove unreacted or unspecifically coordinated radiometal ions [34]. The use of post-labelling purification also provides an opportunity for formulation exchange in the final product, which is sometimes necessary before administration.

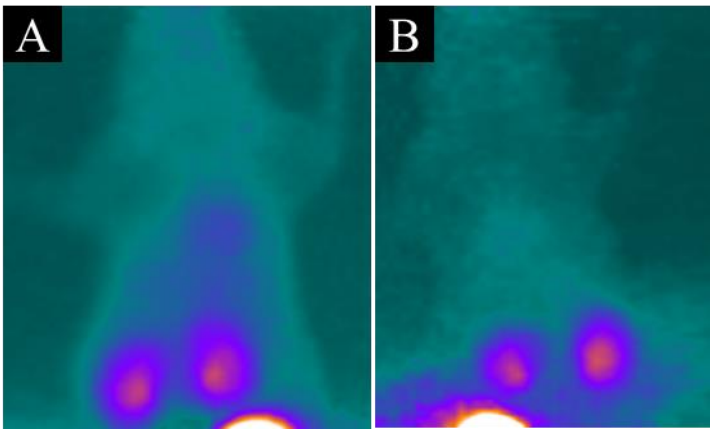

Figure 9. Small animal PET images illustrating different distribution patterns of an injected ^{68}Ga-labelled peptide, when (A) post-labelling purification was excluded and (B) when post-labelling purification was included. All other factors (collection time, injected radioactivity, colour scale, etc.) are equalised between the images. Images from the author's own unpublished data.

1.6.3 Chelating ligands

Radiometal-based radiochemistry relies on coordination chemistry in which a molecule (ligand) donates unshared electrons to a metal ion, i.e. inorganic chemistry. The simplest ligand shares only one pair of electrons and, therefore, forms only one bond to one metal ion. However, many molecules have several unshared pairs of electrons. If they have geometries that permit several pairs of electrons to be donated from different atoms within that molecule to the same metal ion, it is classified as a potential chelating ligand – a so-called chelator [82]. In a chelator-metal ion complex the metal ion is centrally situated, sharing electrons with multiple atoms within the chelator [40,83].

Chelators commonly used in radiopharmaceuticals are usually bifunctional, i.e., in addition to their metal-binding properties, they also have the ability to covalently bind to an appropriate functional group on targeting vectors, molecules such as peptides, nucleotides, antibodies and nanoparticles [84]. Common bonds with chelators are an amide bond between a free carboxylic acid on the chelator and a primary amine on a polypeptide and a thiourea bond between an isothiocyanate (NCS) on the chelator and a primary amine on the polypeptide. These approaches have been used extensively in experimental studies [85,86] as well as in clinical applications [87,88] In 2016 Spang et al [89] predicted a future for kit-based applications of these strategies for labelling clinically-used ^{68}Ga-labelled radiopharmaceuticals, an approach that is very successful today [90,91].

Bifunctional chelators can generally be divided into two groups: macrocyclic and acyclic. Macrocyclic bifunctional chelators are geometrically pre-arranged for their metal ion binding formation, while acyclic bifunctional chelators must undergo a geometrical change when binding to the metal ion. These characteristics make the macrocyclic chelators generally more inert and less flexible with regard to the metal ion size and binding angles. Thus, when the bond between the macrocyclic chelator-metal ion is formed, the complex is generally more stable than that of an acyclic chelator-metal ion complex [84].

Some of the most widely used macrocyclic chelators are 1,4,7,10-tetraazacyclododecane-1,4,7,10-acetic acid (DOTA) and 1,4,7-triazacyclononane-1,4,7-triacetic acid (NOTA). Some of the most widely used acyclic chelators are diethylenetriaminepentaacetic acid (DTPA), ethylenediaminetetraacetic acid (EDTA), N,N-bis(2-hydroxybenzyl)ethylenediamine-N,N-diacetic acid (HBED) and deferoxamine (DFO) [67,92,93].

In this thesis the coordinations of the chelator complexes [^{68}Ga]Ga-DOTA, [^{68}Ga]Ga-NOTA, [^{68}Ga]Ga-HBED and [^{89}Zr]Zr-DFO-NCS are exploited (see Figure 10), as well as the coordination between ^{89}Zr and 8-hydroxyquinoline (oxine) (see Figure 11). The strategy of using bifunctional chelators is often considered metal-nonessential, which means the radiopharmaceutical, or its distribution pattern *in vivo*, will not be very affected by the choice of radiometal. The final structure of complexes coordinating multiple ligands depends on the charge of the radiometal. This may cause a larger variation in distribution patterns *in vivo* depending on choice of radiometal, which means the radiopharmaceutical can be considered

metal-essential [70] (see Figure 11). Although using a bifunctional chelator to label targeting molecules is regarded as a metal-nonessential strategy, differences in the pharmacokinetics and risks of decomplexation *in vivo* may, in individual cases, change it to a metal-essential strategy [93].

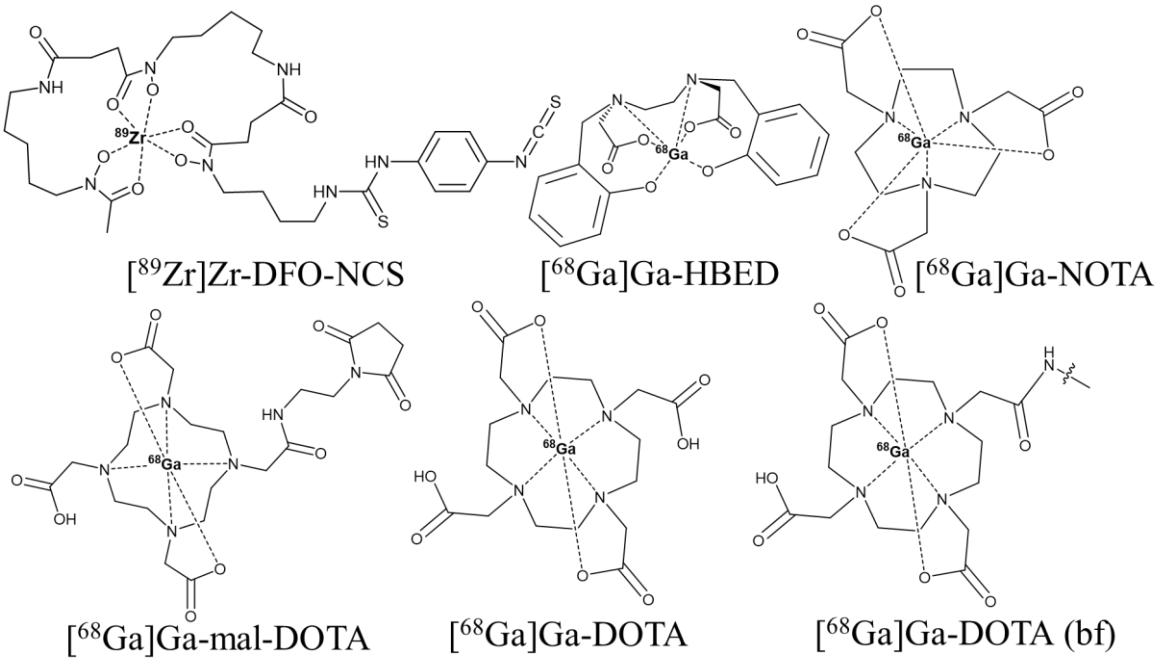

Figure 10. Bifunctional complexes of [^{68}Ga]Ga-mal-DOTA and [^{89}Zr]Zr-DFO-NCS utilised in papers I and II, respectively, of this thesis. The complex [^{68}Ga]Ga-DOTA was utilised in papers III and IV and [^{68}Ga]Ga-NOTA and [^{68}Ga]Ga-HBED and bifunctional (bf) [^{68}Ga]Ga-DOTA in paper IV. The chelator shares its electrons with the metal ion, creating coordinated bonds.

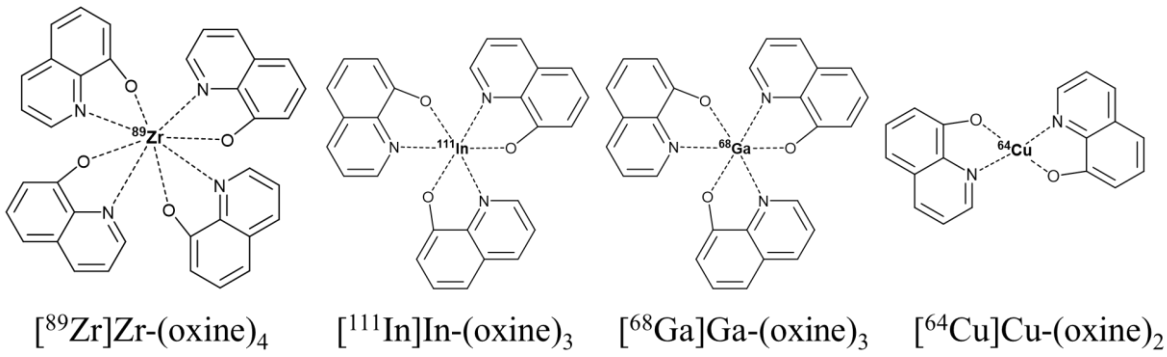

Figure 11. Complexes of [^{89}Zr]Zr-(oxine)$_4$, [^{111}In]In-(oxine)$_3$, [^{68}Ga]Ga-(oxine)$_3$ and [^{64}Cu]Cu-(oxine)$_2$.

Several factors affect the formation of a stable chelator-metal ion complex. Temperature, time and pH are parameters that must be considered when optimising the radiolabelling process [94]. Other factors such as binding angles, size and steric hindrances or protonation/hydrolysation of the chelator/metal ion at different pHs may affect the complexation [95]. Not to be forgotten and of crucial importance is the presence of competing metal ions. Incomplete removal of competing metal ions (e.g. Fe(III) or Zn(II)) in the radiometal production step or introduced in the radiopharmaceutical labelling step (e.g. from poorly cleaned lines or chemicals) will decrease the radiochemical yield (RCY) [96].

When synthesising a new radiometal-based radiopharmaceutical it is important to choose a suitable chelator for the molecule (e.g. biomolecule, pharmaceutical). If the molecule has a slow pharmacokinetics, a radiometal with long half-life is usually preferred. Often acyclic chelators will complex a metal ion more rapidly, which makes them more suitable for labellings with a shorter half-life radiometal for molecules with fast pharmacokinetics. However, it should be considered that chelators with rapid metal ion complexation will most likely also be less stable, which can lead to more rapid decomplexation *in vivo* [40].

If the molecule of interest is heat-sensitive, the chelator must be able to conjugate with both the molecule and the radiometal ion at low temperatures. One such example is the choice of DFO for labelling proteins with ^{89}Zr. The chelator DOTA has been shown to form more stable complexes with ^{89}Zr and thus less decomplexation occurs than with DFO *in vivo* [97]. However, DOTA is seldom used for protein labelling since efficient chelation requires heating at temperatures high enough to destroy many protein structures [41].

1.7 TARGETING MOLECULES AND TRACER DEVELOPMENT

In the field of radionuclide-based molecular imaging, there is a range of different targeting molecules, from small-sized < 0.5 kDa to full-length mAbs of 150 kDa or even larger constructs such as liposomes and nanoparticles. The pharmacokinetics and the optimal time to the peak tissue accumulation depend on many parameters, particularly on the size of the targeting molecules [98]. It is therefore important to match the physical half-life of the radionuclide with the pharmacokinetics of the targeting molecules (see Figure 12). The use of non-standard PET radionuclides [99] is becoming more interesting, particularly for larger molecules. In general, the larger the molecule the slower the pharmacokinetics/-dynamics (the biological half-life).

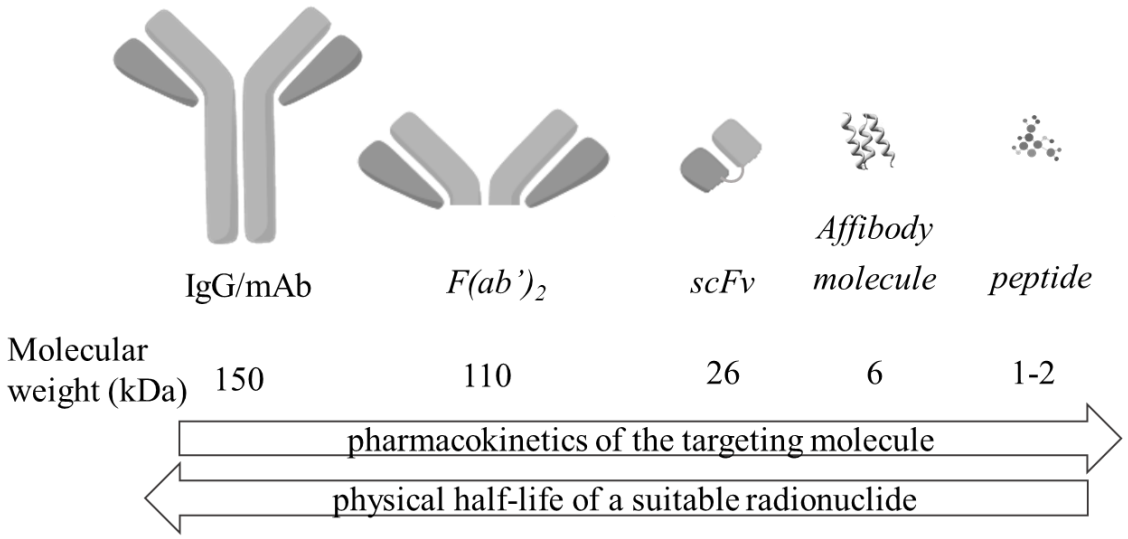

Figure 12. Illustration showing examples of different targeting peptides and proteins, their relation between molecular weight and general pharmacokinetics, and the match with a suitable imaging radionuclide with regard to its physical half-life.

Although the pharmacodynamic fate of the large antibody extends its circulatory half-life, the tumour/target-to-plasma uptake ratio (tumour-to-background uptake ratio in molecular imaging) is not necessarily improved by using a large molecule, since the smaller peptide has a faster uptake in the tumour/targeted tissue. This phenomenon was investigated in a comparison of the full size antibody and antibody fragments of different sizes, down to scFv, for which a U-formed relationship between molecular size and the tumour-to-serum uptake ratio was proposed [100].

The actual half-life of a radiopharmaceutical, the effective half-life, is determined by the biological half-life of the vector molecule and the physical half-life of the radionuclide. See Equation 2.

$$t_{1/2e} = \frac{t_{1/2p} \times t_{1/2b}}{t_{1/2p} + t_{1/2b}}$$

Equation 2. The effective half-life ($t_{1/2e}$) as determined by the biological half-life of the vector molecule ($t_{1/2b}$) and the physical half-life of the radionuclide ($t_{1/2p}$).

The effective half-life is when 50% of the radioactivity has left the biological system (the subject's body in *in vivo* studies). The $t_{1/2e}$ is always shorter than the shorter of the vector molecule's $t_{1/2b}$ and the radionuclide's $t_{1/2p}$ [101]. This illustrates the importance of matching these two parameters, both for dose exposure reasons (valid for both diagnostic and therapeutic

radiopharmaceuticals) and for not interfering with the possibility to detect the intended diagnostic target.

1.7.1 Proteins

In the search for specific targeting molecules for use in radionuclide-based molecular imaging, the endogenous antibodies, such as immunoglobulin G (IgG), are an obvious starting point. These proteins are made in nature for targeting specific biological processes. The mAbs are genetically modified and antigen/target specific selected antibodies. Because of their specificity mAbs have become extremely interesting for the treatment of numerous diseases, especially cancers [44]. To select patients more likely to respond to these treatments it is important to investigate the density and distribution of antigens/targets (e.g. cancer specific expressed receptors) in each individual cancer patient. Stratifying patients using radiolabelled mAbs can also spare non-responding patients unnecessary treatments and related adverse events. Proteins, e.g antibodies, are large molecules with slow pharmacokinetics, which makes radiolabelling with ^{89}Zr suitable for PET imaging. Most often the chelator DFO is chosen because of its capability to complex the radiometal under mild, room temperature conditions, which is necessary to avoid destruction of the large molecule's structure [102]. The approach to stratify patients has already been investigated in clinical trials, e.g. ^{89}Zr-labelled atezolizumab (an anti-programmed death ligand-1 (PD-L1) mAb) [103] and in ^{89}Zr-labelled trastuzumab (an anti-HER2 mAb) [104]. Smaller fragments of antibodies or antibody mimetics, with the antigen/targeting site remaining, have also been investigated.

Peptides are structurally similar to proteins but are much shorter. In the diagnostic setting, a smaller molecule would be favourable due to its more rapid pharmacokinetics, enabling imaging one to a couple of hours after injection instead of after days. An example of this approach is the targeted imaging of HER2 with the diagnostic Affibody molecule ABY-025 to predict the feasibility of antibody HER2+ breast cancer treatment [105].

1.7.2 Affibody molecules

Affibody molecules are engineered polypeptides that are selected for their high affinity binding to different targets *in vivo*. This type of peptide originates from the B-domain in the IgG-binding region of staphylococcal protein A, a 58 amino acid 3-helix folded peptide. Amino acids in the original Fc binding site on helix one and two are altered to gain affinity to, in principle, any biological target protein. Since Affibody molecules are small, and usually expected to display rapid pharmacokinetics, radiolabelling with ^{68}Ga or ^{18}F is suitable for PET imaging. Since these polypeptides generally tolerate higher temperatures there are a number of chelators that can be used for ^{68}Ga-labelling, including the heat requiring chelator DOTA. The chelator is usually conjugated to a single cysteine in the peptide sequence [106]. Affibody molecules have been engineered against several biological targets, such as the most prominent ones targeting HER2 [19,107], human epidermal growth factor receptor 3 (HER3), epidermal growth factor receptor (EGFR) and insulin-like growth factor 1 receptor (IGF-1R) [108], all with high affinities.

1.7.3 Smaller peptides

DOTATOC (DOTA-D-Phe1-Tyr3-octreotide, also edotreotide) is an octreotide derivative, which consists of an 8 amino acid peptide linked to the chelator DOTA. See Figure 13. DOTATOC is an agonist that binds to SSTR, especially type 2, on the cell membrane of NET. [^{68}Ga]Ga-DOTATOC was first described and proposed as a promising SSTR radiopharmaceutical in 2001 [109]. Today [^{68}Ga]Ga-DOTATOC is a clinically approved ^{68}Ga-labelled radiopharmaceutical [17].

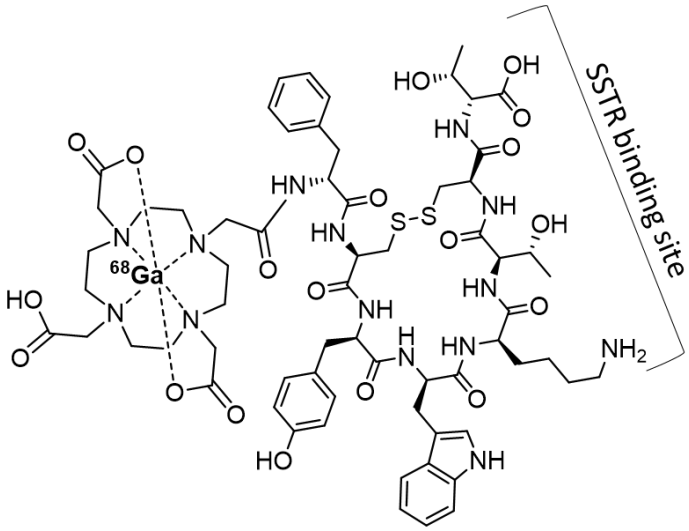

Figure 13. Structure of [^{68}Ga]Ga-DOTATOC with the SSTR binding site.

Following in the footsteps of [^{68}Ga]Ga-DOTATOC, HBED-chelated [^{68}Ga]Ga-PSMA-11, has become a widely used diagnostic tool for imaging prostate-specific membrane antigen (PSMA) positive tumours [81] and is also approved for clinical use in many countries [110]. PSMA expression is found in almost all PCs, with levels increasing with the cancer aggressiveness. To enable PET imaging of PC in earlier stages when PSMA levels are low, a gastrin releasing peptide receptor antagonist has been suggested, e.g. the bombesin analogue DOTA or NOTA-chelated [^{68}Ga]Ga-RM26 [111,112]. [^{68}Ga]Ga-PSMA-11 and [^{68}Ga]Ga-RM26 have been observed to show inverse accumulations during PC progression, which doesn't favour one or the other but rather makes them complementary [111].

The growing awareness that cancer should not be considered as solely the growth of individual proliferating cancer cells but rather a much complex composition including the cells and their microenvironment, has led to an interest in developing radiopharmaceuticals targeting the fibroblast activating protein (FAP) [113,114]. Among other stromal cells co-existing in tumours, such as vascular and immune cells, fibroblasts represent a significant mass of the tumour microenvironment. FAP-inhibitors radiolabelled with ^{68}Ga or ^{18}F have been suggested as promising imaging candidates [115].

1.8 THERANOSTICS

Theranostics link diagnostics to therapeutics, with the aim of refining personalised health care. For radiopharmaceuticals alone to fulfil the theranostic definition, the same molecule is labelled with either a diagnostic or a therapeutic radionuclide. The diagnostic radiopharmaceutical can then be used to predict the feasibility of the suggested radionuclide therapy or immunotherapy and/or to evaluate treatment effects [32].

A number of radiometals have more than one isotope suitable for molecular imaging and/or peptide receptor radionuclide therapy (e.g. $^{60/61/62/64}$Cu, $^{66/67/68}$Ga, $^{86/90}$Y). Isotopes of the same element possess the same charge and chemical properties, which means they will show the same behaviour in labelling procedures and the radiopharmaceutical will have the same distribution patterns *in vivo* [84]. To create a true theranostic pair, a suitable diagnostic isotope and a suitable therapeutic isotope of the same element would be used. One such example is the use of the positron-emitting ^{86}Y and the beta-emitting ^{90}Y [116]. In this case an exact prediction about the biodistribution of the therapeutic could be translated from that of the diagnostic. A good radiodiagnostic match is important, since ^{90}Y doesn't itself emit externally detectable radiation in its decay. Another widely used therapeutic radionuclide, the beta-emitting ^{177}Lu, also emits gamma photons. Dose calculations could thus be made from the therapeutic treatment itself [117]. However, it would not be feasible or, for that matter ethical for dose exposure reasons, to use ^{177}Lu as a diagnostic agent [118]. Instead, the positron-emitting ^{68}Ga can be used as a corresponding diagnostic radionuclide. One such example is the successfully used theranostic pair [^{68}Ga]Ga-DOTATATE and [^{177}Lu]Lu-DOTATATE [119]. Even the not as obvious pair [^{68}Ga]Ga-DOTATOC and [^{177}Lu]Lu-DOTATATE are generally accepted as theranostics [17]. Also, switching from the beta-emitting radionuclide to a high energy alpha-emitting radionuclide, e.g. using the corresponding theranostic pair [^{68}Ga]Ga-DOTATOC and [actinium-225]([^{225}Ac])Ac-DOTATOC, has shown promising results in ongoing studies [120].

The combination of a diagnostic and a therapeutic agent, the concept of theranostics, does not necessarily have to be limited to radiopharmaceuticals alone. Theranostic pairs can consist of e.g. a therapeutic antibody or cell in combination with a corresponding diagnostic radiopharmaceutical [118]. The approach to stratify patients for treatment (earlier described in 1.7.1) can be considered for a theranostic pair, e.g. diagnostic ^{89}Zr-labelled atezolizumab/treatment with atezolizumab [103] and in ^{89}Zr-labelled trastuzumab/treatment with trastuzumab [104].

1.9 CELL RADIOLABELLING

Cell radiolabelling is not new in the field of radionuclide-based nuclear imaging, and over the years it has been applied to many types of cells. The most commonly used is the radiolabelling of leukocytes (WBCs) with ^{99m}Tc or ^{111}In to investigate the presence of infection or inflammation [121,122]. Also radiolabelling of erythrocytes (RBCs) with ^{99m}Tc has been performed for many years for cardiovascular imaging, blood-pool imaging, as denatured for

splenic function imaging [123-125] or gastrointestinal bleeding [126]. Blood-cell radiolabelling is commonly used in clinical nuclear medicine. These routine investigations of diagnostic blood-cell distributions are relatively fast and have established protocols and guidelines regarding the handling and radiolabelling of the cells [122,127].

Like antibody immunotherapy, cell-based immunotherapy is an emerging field of interest in oncology. The fundamental purpose of immunotherapy is to modify and enhance the host immune system to infiltrate the cancer microenvironment and to recognise specific cancer associated antigens, with the end goal to fight cancer cells. Normally, the recognition and elimination of cancer cells are dealt with by the host immune system itself, but in the cancer patient some of these functions are deficient or lost [128]. The development of new anti-cancer cell therapy approaches is steadily in progress, including research on T cells and how they interact with other immune cells, such as natural killer (NK) cells, dendritic cells (DCs), and macrophages in the tumour development. Interest in using stem cells for therapy has also increased. To gain more knowledge about the migration and homing, the overall behaviour of the cells after injection/transplantation, it is of importance to find methods to track the cells *in vivo* and over time [129,130].

1.9.1 Direct cell labelling

In contrast to radiopharmaceuticals injected to track biological targets or processes *in vivo*, direct *in vitro* cell radiolabelling does not have to be cell/target specific, since the cells can be separated during the labelling procedure. An important criterion, though, is that the radioactivity be fixed inside/to the cells for a sufficient time to allow for imaging, i.e. a "trapping" mechanism must exist.

The method often used to radiolabel RBCs is based on "pretinning" the cells to trap the radioactivity intracellularly by the reduction by tin of ^{99m}Tc, from the negatively charged pertechnetate ($Tc^{7+}O_4^-$) to the positively charged and metal-complex coordination capable Tc^{4+} [123]. In this radiolabelling method Tc^{4+} coordinates to the β-globin chains of haemoglobin inside the RBCs. The "pretinning" and radiolabelling procedures with RBCs have been performed both *in vivo* and *in vitro*, with the latter method shown to be more successful for imaging quality [125].

Leukocytes (WBCs) possess no haemoglobin, which is also true for all cells except the RBCs. For this reason, the radiolabelling method described above cannot be used. Other methods have therefore been developed and used to radiolabel WBCs as well as a variety of other cells.

Cell labellings often use [^{99m}Tc]Tc-hexamethylpropyleneamine oxime ([^{99m}Tc]Tc-HMPAO) (see structure in Figure 14) or [^{111}In]In-(oxine)$_3$ (see structure in Figure 11) for gamma/SPECT imaging. Since these compounds are small and highly lipophilic, they should passively diffuse through the cell membrane.

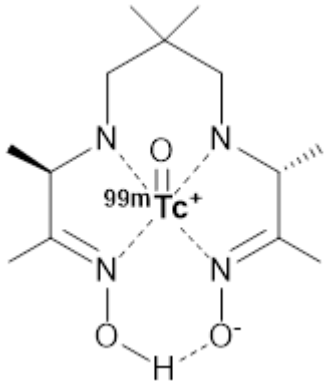

Figure 14. The small lipophilic complex, [^{99m}Tc]Tc-HMPAO.

The cell trapping mechanism for [^{99m}Tc]Tc-HMPAO is suggested to depend on the reduction of the radiopharmaceutical to a more hydrophilic form, which prevents it from passively diffusing back to the extracellular compartment. A reducing agent such as glutathione, which is found in high concentrations intracellularly but in low concentrations extracellularly, is suggested to be responsible for this action [131].

The cell trapping mechanism for [^{111}In]In-(oxine)$_3$ is due to the low coordination stability constant between the three oxine ligands and the $^{111}In^{3+}$ metal ion, compared to intracellular components that can coordinate the metal ion with higher stability constants. In this exchange reaction the lipophilic oxine ligands are passively diffused through the cell membrane to the extracellular compartment, while the radioactivity (^{111}In) is trapped intracellularly [122].

The use of small lipophilic compounds when radiolabelling is not selective for a certain type of cell and can therefore be applied in the radiolabelling of any type of cell. Both WBCs and RBCs, as well as a wide variety of other cells, have been radiolabelled with e.g. [^{111}In]In-(oxine)$_3$ [132] as well as its PET counterparts [^{68}Ga]Ga-(oxine)$_3$ [132,133], [^{64}Cu]Cu-(oxine)$_2$ and [^{89}Zr]Zr-(oxine)$_4$ [132]. The final structure of these complexes depends on the charge of the radiometal, which means the radiopharmaceutical can be considered metal-essential (see Figure 11).

Also 2-[^{18}F]FDG has been used to radiolabel cells for PET imaging [134]. It is taken up by the GLUT transporter. Its widely known cell trapping mechanism functions as the cell radiolabelling function [135].

A third alternative to the passive diffusion and transporter mediated uptake mechanisms is the binding of the radionuclide-carrying complexes to the cell membrane surface. This method utilises (as in e.g. [^{89}Zr]Zr-DFO-NCS [7]) the complex capacity to bind to free amines on cell surface proteins. This alternative method is suggested to be more robust than the other two direct labelling techniques, circumventing the risk of leakage from cells often seen in intracellular direct radiolabelling [7,130].

In paper II two different *in vitro* cell radiolabelling techniques were explored, passive diffusion through the cell membrane using [^{89}Zr]Zr-(oxine)$_4$ and binding to the cell membrane using [^{89}Zr]Zr-DFO-NCS. See Figure 15.

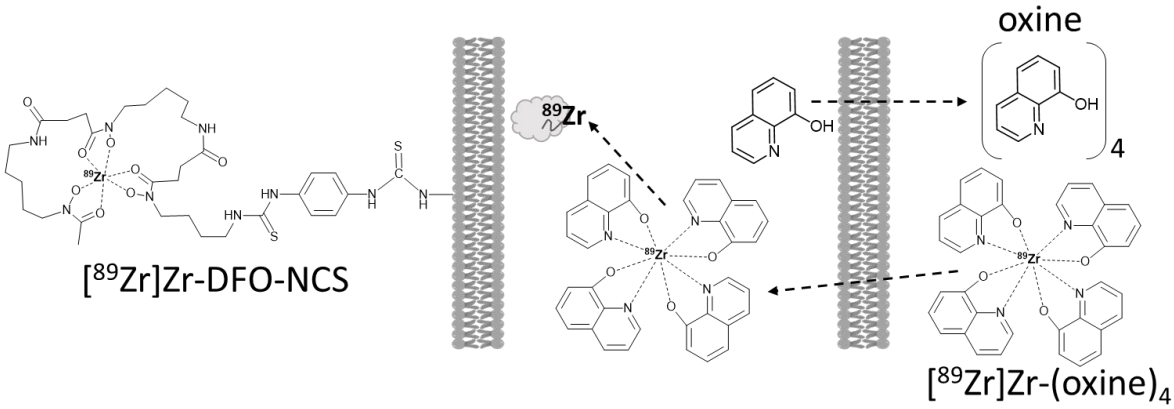

Figure 15. In vitro cell labelling techniques explored in paper II.

1.9.2 Indirect cell labelling

Indirect cell labelling is based on the incorporation of so-called reporter genes into the cells' deoxyribonucleic acid (DNA). These genes are transcribed to proteins (such as enzymes, receptors, or transporters), which in turn can be targeted by a radiopharmaceutical compound. The indirect targeting approach means the cells are labelled *in situ* after administration [130].

Using this technique, it is not necessary to use a long-lived radionuclide when long-term tracking of cells is desired, as the patient/animal can be re-examined with a new radiopharmaceutical administration at certain time points after administration of the cells. This is true if a radiopharmaceutical with fast pharmacokinetics (e.g. small molecule, peptide) is used, while a radiopharmaceutical with slow pharmacokinetics would still require a long-lived radionuclide.

The most frequently used reporter gene in radionuclide-based cell tracking imaging is the herpes virus type 1 thymidine kinase (HSV1-tk), *in situ* radiolabelled with 9-[4-[^{18}F]fluoro-3-(hydroxymethyl)butyl]guanine ([^{18}F]FHBG) [136]. Reporter genes transcribing receptors such as PSMA and SSTR2 have also been suggested [136,137], potentially as *in situ* targets for the commonly used radiopharmaceuticals [^{68}Ga]Ga-PSMA/[^{18}F]PSMA and [^{68}Ga]Ga-DOTATOC, respectively.

1.10 EVALUATION OF THE RADIOLABELLED TRACER

In the process of evaluating a new radiopharmaceutical there are an array of assays to be performed for predicting and determining its possible future success as a radionuclide-based molecular imaging tool. Each step in the process needs to be evaluated carefully to justify further progression. Assuming the chemical characteristics of the molecule (i.e. precursor compound) and its binding capacity to a biological target have been calculated, the next steps involve confirmation using *in vitro* and *in vivo* assays. In other words, each radiopharmaceutical must be evaluated to confirm its actual pharmacokinetics and pharmacodynamics [93,138].

1.10.1 *In vitro* assays

Evaluation of the radiopharmaceutical's/radiotracer's capacity to bind to its intended target is first performed using *in vitro* assays. These assays can consist of either an immobilised target on enzyme-linked immunosorbent assay (ELISA) plates [139], cell cultures expressing the target or on tissue sections.

In these assays it is confirmed whether or not the radiotracer is capable of binding to its intended target. These assays lack information about the radiotracer's capability to cross biological barriers, e.g. the blood-brain barrier (BBB) or barriers as a result of the tumour microenvironment in solid tumours. To better mimic the latter, three-dimensional (3D) cell culture systems have been developed [140].

In paper I ELISA plates were coated with the biological target and incubated with the radiotracer. The plates were subsequently exposed to phosphor crystal plates and scanned using a phosphor imager to estimate the equilibrium binding constant (Kd), the binding capacity, of the radiotracer.

In paper II cell cultures were radiolabelled using the two different radiotracers to evaluate the binding/uptake capacity and the efflux over time. The possible effects of radiolabellings on the phenotypes of the cells were examined by flow cytometry.

1.10.2 *In vivo* evaluations

The second step in the evaluation of the radiopharmaceutical's/radiotracer's capacity to reach and bind to its intended target is performed in suitable animal models. These models are designed to mimic human conditions and diseases to enable the study of human biology and genetics and for the preclinical evaluation of pharmaceuticals (including radiopharmaceuticals). Cancer models have been generated from graft transplantations (e.g. xenografts) or by genetic engineering. Other types of models have been generated by viral, chemical or physical induction [141].

In addition to target binding, information regarding biodistribution, pharmacokinetics, pharmacodynamics and dosimetry is obtained in the animal experiments. Radionuclide-based molecular imaging is an excellent example of a technique that implements the principle of humane experimental study design. This principle emphasises the importance of animal

welfare and reducing the number of animals used in experiments to a minimum, which can be achieved by the replacement to non-sentient alternatives and/or the refinement of the study design, the 3 Rs [142]. The non-invasive nature of the imaging procedure and the microdosing of the radiopharmaceutical are well in line with the 3 Rs principles, generating tremendous amounts of quantitative data using a low number of animals.

In paper I of this thesis different animal cancer/naïve models and a physical induction model were used to evaluate the investigated radiotracers' *in vivo* behaviour, using a small animal PET camera. Ethical permits were followed during all experiments in this study. For animal health and well being, the Karolinska Institutet's guidelines for animal handling and monitoring were followed.

1.11 CLINICAL TRANSLATION ASPECTS OF RADIOPHARMACEUTICALS

As indicated by its name, a preclinical study aims to prepare/determine feasibility for a possible clinical trial. The study often includes investigations of safety (e.g. toxicology and dosimetry) and biology (e.g. pharmacokinetics and targeting capability) of the radiopharmaceutical compound. When the developed and preclinically evaluated radiopharmaceutical is to be translated from the preclinical stage to a clinical trial, there are many aspects to be considered. The productions of radiopharmaceuticals for human use are regulated by directives, regulations, and rules [143]. These describe how good manufacturing practice (GMP) and good laboratory practice (GLP) are to be implemented in the production of the radiopharmaceutical production. More precisely, there are descriptions of how the documentation and responsibility systems within the small-scale radiopharmacy are to be conducted, as well as the handling of materials, staff education, environmental, validation, preparation/synthesis and quality control requirements.

A radiopharmaceutical included in a clinical trial is considered an Investigational Medical Product (IMP) and is described in the clinical trial all-inclusive documentation, the Investigational Medical Product Dossier (IMPD). The rigorous documentation and validation requirements to the IMP can be a decisive hurdle, which has been reflected in the decreasing numbers of clinical trial applications in the past years [144,145]. With the updated guidelines on good radiopharmacy practice (cGRPP), an adaptation to the small-scale preparations/productions of radiopharmaceuticals has been implemented [143], with the aim of reducing this hurdle and harmonising interpretations of the directives, regulations, and rules among the European Union countries [143,145].

2 AIMS OF THIS THESIS

The overall aim of this thesis is to develop radiometal-based labelling techniques and tracers for non-invasive molecular imaging.

Specific aims include:

- To develop and evaluate a ^{68}Ga-labelled polypeptide for non-invasive *in vivo* molecular imaging of albumin distribution.
- To optimise the cyclotron production of ^{68}Ga using a solid target on a cyclotron and
- To evaluate the usefulness of cyclotron-produced ^{68}Ga for labelling clinically relevant tracers.
- To develop long-lived ^{89}Zr-based tracers for cell labelling.

3 METHODS, RESULTS AND DISCUSSIONS

3.1 RADIOLABELLING AND *IN VIVO* EVALUATION OF [^{68}Ga]Ga-ABY-028 (PAPER I)

In paper I an albumin-binding probe was developed and evaluated. ^{68}Ga was obtained from commercially available ^{68}Ge/^{68}Ga generators (IGG-100 or GalliaPharm, Eckert & Ziegler). Using this readily available route to the radiometal, the study focused on concentrating the generator eluate (see Figure 17) to achieve successful labelling of a medium-sized polypeptide and evaluating the radiolabelled product's *in vivo* imaging behaviour. The radiolabelled polypeptide was the Affibody molecule [^{68}Ga]Ga-ABY-028. The overall hypothesis for the PET applications was that albumin-binding [^{68}Ga]Ga-ABY-028 can be used to trace the distribution of albumin *in vivo*. Sub-hypotheses formed were that the albumin-bound tracer can be used to differentiate vascular properties and to characterise tissue permeability, also with a potential for its use as baseline for the uptake of albumin binding domain (ABD)-based macromolecular diagnostics and therapeutics.

The Affibody molecule was produced by solid phase peptide synthesis and coupled to the chelator 1,4,7,10-tetraazacyclododecane-1,4,7-tris-acetic acid-10-maleimidoethylacetamide (mal-DOTA). Site-specific direction of the radiolabelling was achieved by coupling the mal-DOTA chelator through a thiol in the single cysteine of the Affibody molecule. See Figure 16.

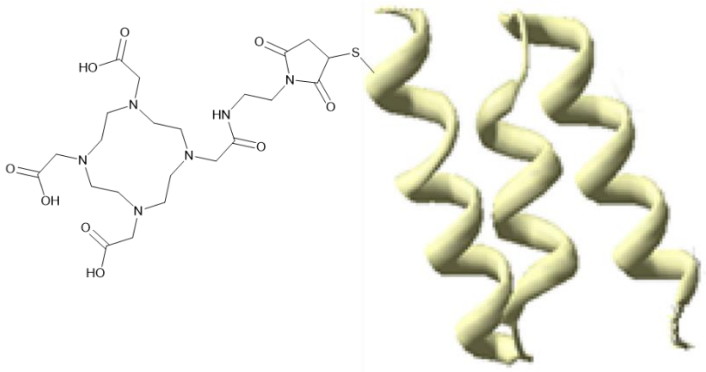

Figure 16. ABY-028 with the chelator mal-DOTA coupled through a thiol in the single cysteine of the Affibody molecule.

The ^{68}Ga-eluate was concentrated using the Chromafix 30-PS-HCO_3/HCl [146], Bond Elut-SCX/NaCl [147] and fractionation [148] (also see Figure 17) methods. The first two methods yielded lower amounts of isolated ^{68}Ga or it was obtained in a medium incompatible with the polypeptide, respectively. Fractionated ^{68}Ga-eluate was adjusted to pH 4.0 by using NaOAc buffer. Ethanol was added to the reaction solution to minimise radiolysis. The ^{68}Ga solution was then transferred to a vial containing freeze-dried ABY-028 and heated to accomplish the radiolabelling. EDTA was used to chelate unreacted/unspecifically bound ^{68}Ga. The crude

product was purified using a solid phase extraction (SPE) column, resulting in a final product with a RCY of ~80% and with a radiochemical purity (RCP) of ~95%.

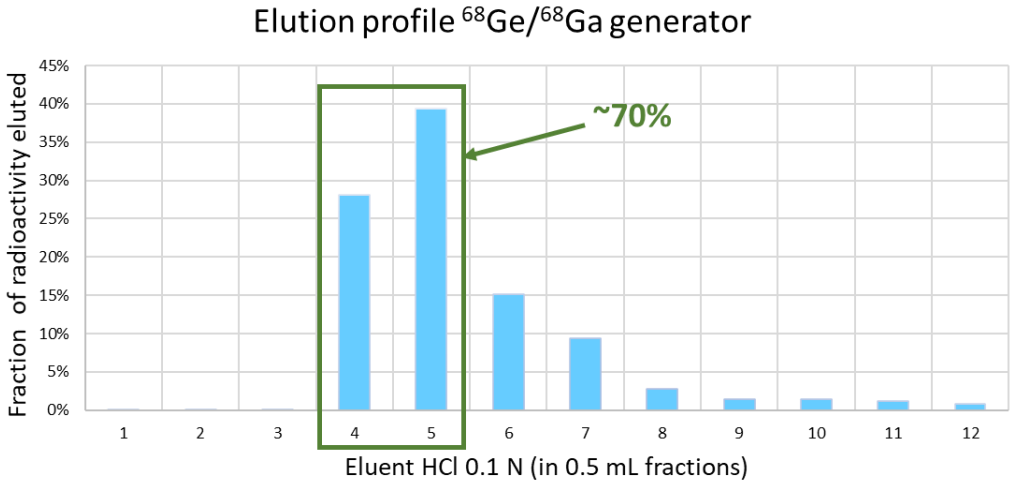

Figure 17. A fractionated generator elution method was used to concentrate the ^{68}Ga-eluate used for labelling of ABY-028 in paper I. Approximately 70% of the total radioactivity was collected in 1 mL of eluate.

Immobilised human serum albumin (HSA) on ELISA plates, analysed by PI, was used to investigate if the albumin binding capability of ABY-028 was retained after ^{68}Ga-labelling. Different concentrations of [^{68}Ga]Ga-ABY-028 (with or without blocking with unlabelled ABY-028) were utilised to study the specificity to HSA. Results showed a specific binding to HSA of 3.4 ± 0.1 nM, indicating the albumin binding capacity was retained after radiolabelling.

The radioactivity distribution patterns, after intravenous (i.v.) injection of [^{68}Ga]Ga-ABY-028, were analysed in healthy rodents using a small animal PET camera (microPET Focus 120®, Siemens/CTI Concorde MicroSystems) which was used for all *in vivo* studies. The radioactivity distributions in both rats and mice were consistent with the expected rapid and persistent binding of [^{68}Ga]Ga-ABY-028 to plasma albumin. Most radioactivity was in the circulatory system during the PET scans, with the highest levels in the heart and the major vessels. Radioactivity in blood-rich organs (e.g. liver and spleen), a gradual transport of radioactivity to muscle tissue, and an increased concentration in the urinary bladder were observed over time. The radiotracer's behaviour was subsequently studied in several animal models of cancer.

Xenograft models of human epidermoid carcinoma (A431) and human squamous carcinoma of the hypopharynx (FaDu) in NIH-Foxn1mu rats were compared. A higher uptake of the radiotracer was observed in FaDu than A431 at early time points, but with a gradual decrease

in differences at later times. At 60 min after injection uptake was still 2.5-3 times higher in the FaDu xenografts.

To investigate if the [^{68}Ga]Ga-ABY-028 uptake in tumour could be manipulated, vasodilating nitroglycerin (NG) ointment was applied cutaneously over the A431 xenografts 1 hour after the tracer administration. After an additional hour from the application of the NG the tumour radioactivity levels began increasing more rapidly. However, the levels in the A431 xenografts during the entire 180 min scan never reached those in the FaDu xenografts.

A dual radiotracer ([^{68}Ga]Ga-ABY-028 and 2-[^{18}F]FDG) study was performed in a MMTV-PyMT transgenic mouse model. A tendency to an inverse relationship between the uptake of the two radiotracers was seen in the early PET scan, i.e. the permeability to the albumin-bound [^{68}Ga]Ga-ABY-028 was higher in several lower metabolic parts of the tumour revealed by the 2-[^{18}F]FDG uptake.

To investigate further if the [^{68}Ga]Ga-ABY-028 radiotracer could be used for visualisation of permeability alterations over time in a tumour, a NIH-Foxn1mu rat with two FaDu xenografts were studied and also compared with 2-[^{18}F]FDG. See Figure 18. The inverse relationship between the radiotracers' uptakes was most pronounced in the larger tumour. Overall, uptake patterns of albumin-[^{68}Ga]Ga-ABY-028 were more heterogenous at early and later times than of 2-[^{18}F]FDG, though the differences were less marked at later times.

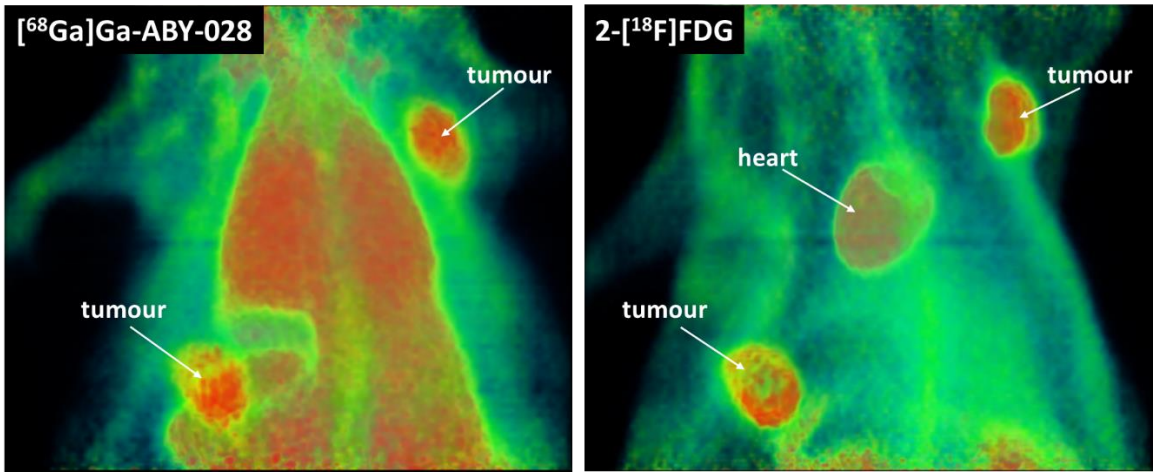

Figure 18. Images showing summarised radiotracer uptake during a 195 min PET scan in a NIH-Foxn1mu rat with two FaDu xenografts. Left: albumin-bound [^{68}Ga]Ga-ABY-028 distribution in the circulatory system and in the permeable tumours. Right: 2-[^{18}F]FDG uptake in the heart and in the high metabolic tumours.

To investigate if the albumin-bound [^{68}Ga]Ga-ABY-028 could be used to visualise increased vascular permeability in cerebral lesions, with an additional question of whether predictions about the uptake of ABD-bound therapeutics might be possible, a model of induced cortical infarction was used [149]. Increased uptake of the albumin-bound [^{68}Ga]Ga-ABY-028 was

observed in the areas of the cerebral infarct, which was also confirmed *ex vivo* by PI of brain sections. Uptake of the radiotracer in brain was not observed in any of the other animals in paper I.

In this study we successfully labelled the mal-DOTA conjugated ABY-028 with ^{68}Ga. We showed that the biodistribution of the radiotracer was consistent with the expected rapid and persistent binding of [^{68}Ga]Ga-ABY-028 to plasma albumin. Uptake patterns in tumours differed at early and later imaging times (indicating the importance of the time window during which the scan is performed) and between tumours at different developmental stages as well as between tumours of different phenotypes (indicative of the importance of the time window for performing the study in dynamic pathological processes). Tracer uptake responses to permeability-altering therapeutic intervention and during the acute phase after cerebral infarction could be observed, for which the dynamic PET imaging capability was important. In summary, this novel radiotracer, the albumin-binding [^{68}Ga]Ga-ABY-028, is a promising tool for *in vivo* molecular imaging of variations and alterations of vascular permeability. The radiotracer has a potential to function as a baseline control of the non-specific uptake of other ABD-based diagnostic or therapeutic agents. The mal-DOTA chelator used here in the labelling by ^{68}Ga is also a suitable chelator for e.g. the more long-lived radiometal ^{89}Zr if studies at later windows of observation are desired.

3.2 ^{89}Zr-LABELLING OF CELLS (PAPER II)

The interest in using cells for therapy has increased. To gain more knowledge about the cells' migration and homing, their overall behaviour after injection/transplantation, it is important to develop methods to track the cells *in vivo* and over time [129,130]. In paper II cyclotron-produced ^{89}Zr was used, two ^{89}Zr-complexes, [^{89}Zr]Zr-(oxine)$_4$ and [^{89}Zr]Zr-DFO-NCS were optimised and subsequently used in a head-to-head comparisons of their cell labelling capabilities.

The two radiolabelled complexes deliver the positron-emitting radionuclide, ^{89}Zr, to the cell in two mechanistically different ways. See Figure 15. [^{89}Zr]Zr-(oxine)$_4$ forms a lipophilic complex capable of passively diffusing through the cell membrane. The coordination stability constant between the four oxine ligands and the $^{89}Zr^{4+}$ metal ion is lower than that of the intracellular components that can coordinate the metal ion. Thus, the complex dissociates intracellularly. In this exchange reaction the lipophilic oxine ligands passively diffuse through the cell membrane to the extracellular compartment, while the radioactivity (^{89}Zr) is trapped intracellularly [45]. The [^{89}Zr]Zr-DFO-NCS complex consists of the chelator DFO, which coordinates to the radiometal. It is also equipped with a NCS group, which can bind to free amines on cell membrane proteins [7].

Radiolabelling optimisations

^{89}Zr was obtained either via an external vendor (PerkinElmer) or produced in-house on a solid-target medical cyclotron (Comecer/GE Healthcare, PETtrace 800) and used in its [^{89}Zr]Zr-(oxalate)$_4$ form without further modification for the radiosyntheses.

Synthesis protocols were optimised to yield [^{89}Zr]Zr-(oxine)$_4$ and [^{89}Zr]Zr-DFO-NCS with high radiochemical conversions (RCC) of 98.4% and 98.0%, respectively. See Table 4. The optimisations included choice of buffers, temperatures and concentrations. See Figure 19. Possible toxic effects of oxine and DFO-NCS on the cells were evaluated and the radiosynthesis protocols were adjusted accordingly.

With such high RCCs a final purification process could be excluded, which saved time and unnecessary radiation doses to the operator. The RCCs were consequently the same as the final radiochemical purities (RCPs) of the ^{89}Zr-complexes used for the subsequent cell labelling procedures.

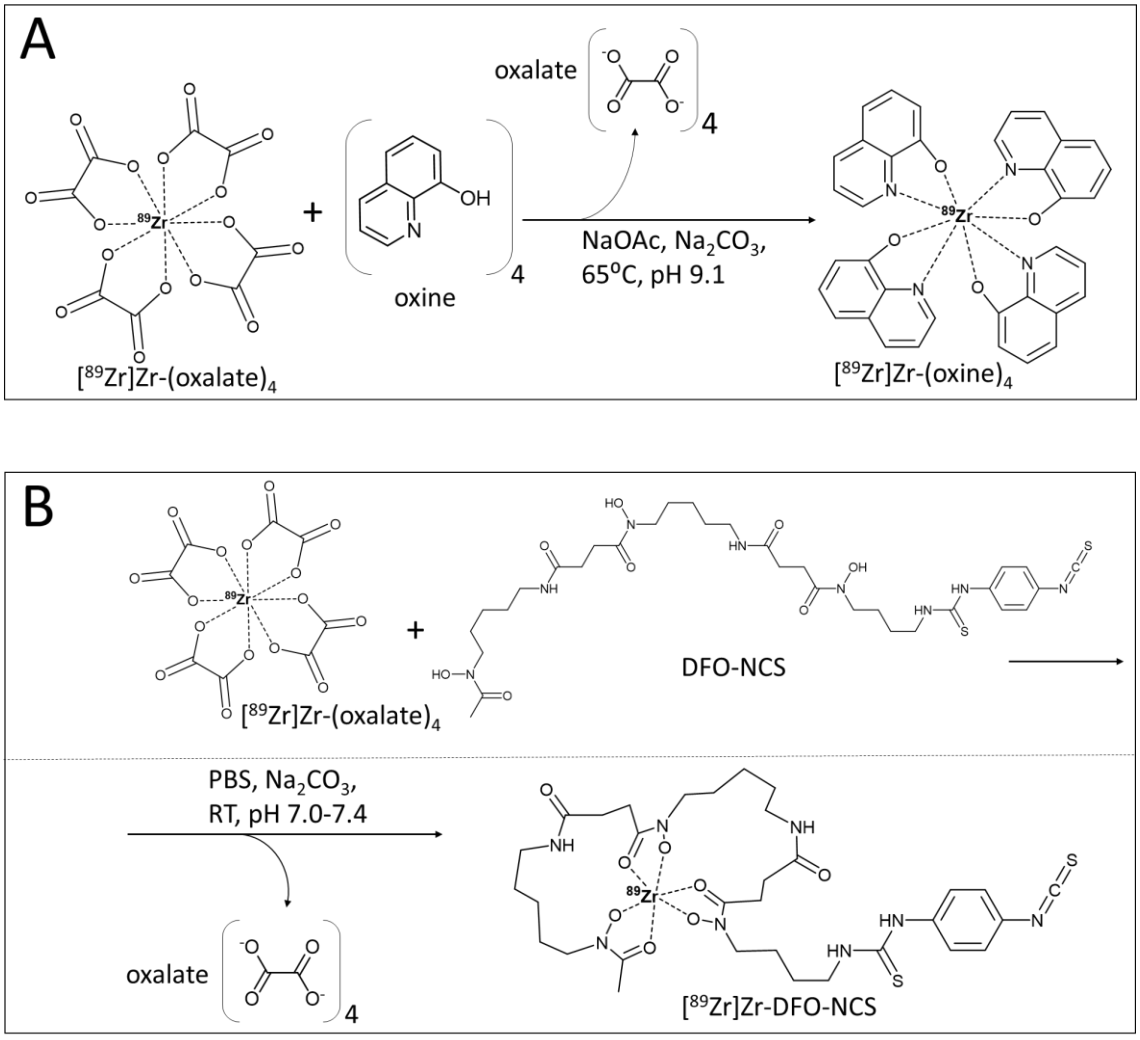

Figure 19. Radiosyntheses of (A) [^{89}Zr]Zr-(oxine)$_4$ and (B) [^{89}Zr]Zr-DFO-NCS in paper II.

The ^{89}Zr-complexes were evaluated with respect to their cell labelling efficiencies (CLE) and cell retention capabilities in three different cell types: human Decidual Stromal Cells (hDSCs), rat bone marrow derived Macrophages (rMac), and human Peripheral Blood Mononuclear Cells (hPBMCs). These cells were selected because of their structural differences, which allowed us to study the theoretically possible universality of labelling strategies using these ^{89}Zr-complexes. The interest in using these types of cells in cell tracking studies is well documented [129,130].

The shelf-lives of the ^{89}Zr-complexes for i.e. how long in advance the radiosyntheses could be performed before cell labellings were investigated. For [^{89}Zr]Zr-(oxine)$_4$ no change in CLE was observed during the entire 7 days of testing. For [^{89}Zr]Zr-DFO-NCS a distinct drop in CLE was observed already 1 – 1.5 hours after radiosynthesis. The distinct drop in shelf-life for [^{89}Zr]Zr-DFO-NCS is suggested to likely depend on hydrolysation of the NCS group over time. When performing the cell labelling directly after the radiosyntheses no significant differences in CLE between the labelling methodologies or between the cell types were observed. See Table 4.

Table 4. Results from the syntheses and cell labelling efficiencies (initial and over time), of [^{89}Zr]Zr-(oxine)$_4$ and [^{89}Zr]Zr-DFO-NCS.

	[^{89}Zr]Zr-(oxine)$_4$ (n = 15)	**[^{89}Zr]Zr-DFO-NCS (n = 13)**
RCC/RCP (%)	98.4 ± 1.3	98 ± 0.6
CLE (%)	60.9 ± 4.2	69.7 ± 8.0
CLE Stability time	≤ 7 days	≤ 1.5 hours

One important reason for using ^{89}Zr in cell labelling is that the relatively long half-life of the radionuclide allows *in vivo* cell tracking during 2 – 3 weeks [7]. For that reason, the stability of the ^{89}Zr-complexes and their intracellular retentions capability were evaluated at early (24 h) and late (7 days) times. For [^{89}Zr]Zr-(oxine)$_4$ no significant differences between the cell types were observed regarding retention capability during the 7 days of measurement. The loss of retention was minimal between early and late times when radiolabelling with [^{89}Zr]Zr-(oxine)$_4$. For [^{89}Zr]Zr-DFO-NCS the retention differed between the cell types at both the early and the late measurements and loss of retention over time were seen in two cell types, rMacs and hPBMCs.

Functional evaluation

Several functional assays were performed on the cells in order to investigate possible effects the radiolabelling might have on the cells as compared to unlabelled cells. These parameters include cell viability, cell proliferation rate, phenotype and/or phagocytosis

The cell proliferation rate and viability for the radiolabelled and non-radiolabelled cells were compared. No significant differences were observed for any of the cell types, independent of the labelling method. Assessment of whether the phenotype of the hDSCs was sustained after radiolabelling by antigen expression using flow cytometry showed that cell type specific antigens were sustained but with a slightly altered composition. Functional control of the rMacs between radiolabelled or unradiolabelled cells compared by phagocytic function using flow cytometry showed a small but significant decrease for the radiolabelled cells. Both phenotype and phagocytic function results were independent of radiolabelling method.

We optimised the radiosynthesis of both [^{89}Zr]Zr-(oxine)$_4$ and [^{89}Zr]Zr-DFO-NCS with similar results regarding RCC and CLE. A very important optimisation of the [^{89}Zr]Zr-(oxine)$_4$ synthesis was the avoidance of the cumbersome liquid-liquid extraction methods previously described [150]. The method used here is more in line with the preparation of the in-human-use approved [^{111}In]In-(oxine)$_3$ [122] from the radiopharmacy's point of view, which may simplify the translation to [^{89}Zr]Zr-(oxine)$_4$ in many ways.

Both cell radiolabelling methods presented in our study indicate relatively universal *in vitro* radiolabellings of different cell types, with [^{89}Zr]Zr-(oxine)$_4$ being superior. Differences in retention of the radiolabel when [^{89}Zr]Zr-DFO-NCS was used are suggested to likely depend on the cell type specific expression levels of proteins containing amine groups on the cell membranes, as well as other cell specific characteristics.

This head-to-head comparison reveals the advantages and disadvantages of cell labelling methods using [^{89}Zr]Zr-(oxine)$_4$ and [^{89}Zr]Zr-DFO-NCS. The radiosynthesis of [^{89}Zr]Zr-DFO-NCS is somewhat faster, but [^{89}Zr]Zr-(oxine)$_4$ had a significantly longer shelf-life. [^{89}Zr]Zr-(oxine)$_4$ also showed to be a more universal cell labelling approach, with less discrimination between the cell types regarding the retention capacity.

3.3 CYCLOTRON PRODUCTION AND PURIFICATION OF ^{68}Ga (PAPER III)

In paper III an automated cyclotron production method and a purification method for clinically useful ^{68}Ga were developed. With the increasing demand for ^{68}Ga for clinical use and the relatively low amounts that can currently be eluted from commercial ^{68}Ge/^{68}Ga generators there is a need to develop alternative production routes for the radiometal. With the solid-target cyclotron production route large amounts of ^{68}Ga may be produced.

Enriched zinc-68 (^{68}Zn) foils were transferred using a Comecer EDS system to the irradiation station Comecer PTS and irradiated using a GE Healthcare (PETtrace 800) cyclotron. To

reduce the amount of unwanted and long-lived ^{67}Ga in the product, a degradation foil was used to decrease the energy of the bombarding protons. After 68 min bombardment with 25 µA protons, ^{68}Ga, produced through the ^{68}Zn(p,n)^{68}Ga reaction, was 31 ± 1 GBq, as measured in the foil and calculated to EOB.

After the irradiation, the foil was automatically transferred to the dissolution station (Comecer EDS) and subsequently the dissolved foil/metal solution was transferred to the cassette-based purification module (Comecer Taddeo PRF). The solution was purified using anion exchange Uranium and TEtraValents Actinides (UTEVA) resins. Different concentrations of HCl were used to optimise the retention of the ^{68}Ga and remove unwanted chelating competitive metal ions. A last wash solution of 2.5 N HCl was included in the final protocol to remove most of the zinc (Zn) and iron (Fe) ions. See Figure 20 and 21. A decay-corrected recovery of 76 ± 8% of the ^{68}Ga produced in the foil could be obtained in the final solution.

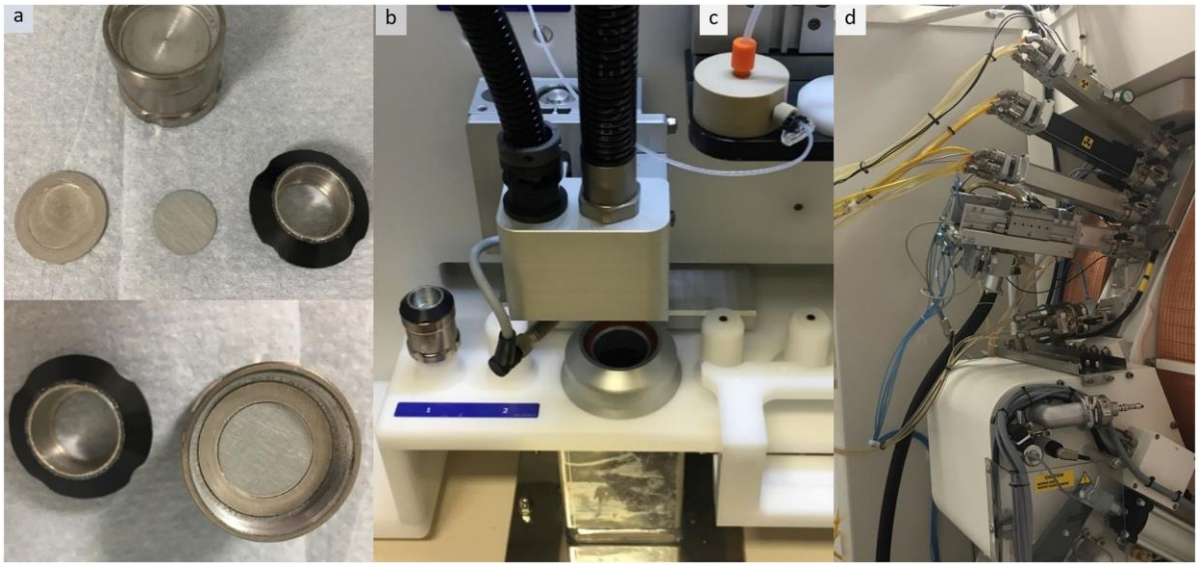

Figure 20. Target set-up for the production of ^{68}Ga in paper III (and IV) including: (a) enriched ^{68}Zn foil and shuttle (b) transfer system between hot cell and cyclotron (c) lid for the returning shuttle for transfer of dissolution acids (d) solid target irradiation station mounted on the cyclotron. Figure from paper III.

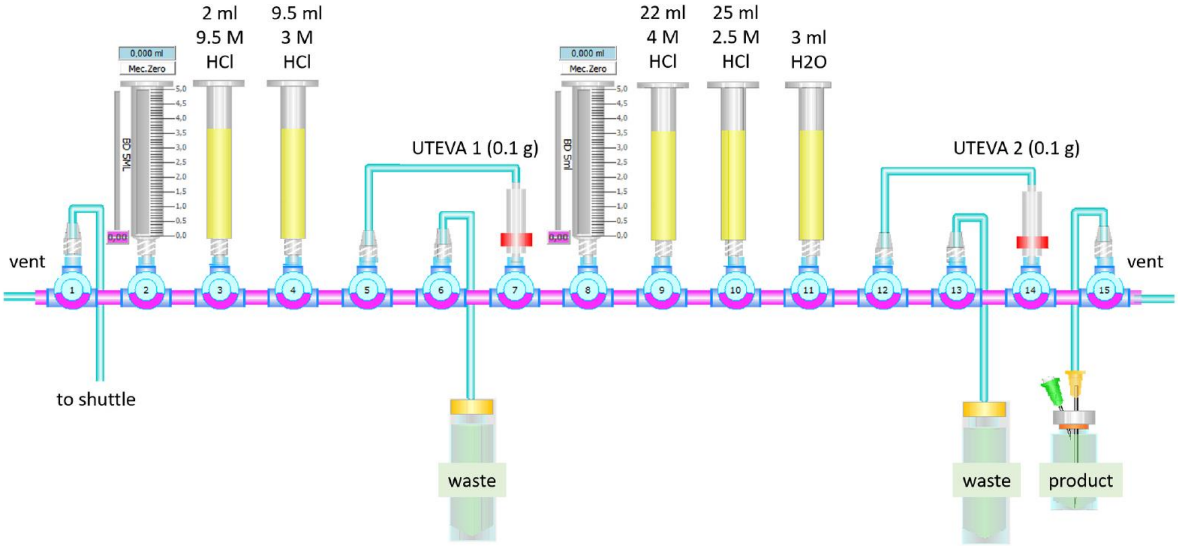

Figure 21. The cassette set-up used in the final protocol for purifying the solid target cyclotron-produced ^{68}Ga. Figure from paper III.

RNP analysed by gamma-spectroscopy (Canberra), was 99.98%. Contents of two other radioactive Ga-isotopes, gallium-66 (^{66}Ga) and ^{67}Ga, were well below the limits required in the European Pharmacopoeia (Eur Pharm) Monograph for accelerator-produced ^{68}Ga [151]: 0.010% and 0.015% respectively. The half-life of the product was measured to 67.8 minutes using a dose calibrator (Capintec). Metal analysis by Inductively Coupled Plasma-Mass Spectrometry (ICP-MS) showed values for e.g. Zn and Fe of 0.0053 µg/GBq and 0.011 µg/GBq at EOB, respectively. The A_m and A_s were calculated from the sum of Ga ions measured by ICP-MS plus the ^{68}Ga obtained in the production, divided by radioactivity obtained in the product. A_m and A_s were estimated to be 102,310 GBq/µmol and 1502 GBq/µmol at EOB, respectively, close to the maximum theoretical values. The apparent molar activity (AMA) was estimated by titrations with the chelator DOTA, showing a value of 86 ± 22 GBq/µmol at EOB. The values of A_m, A_s, AMA, and metal (Zn and Fe) to activity ratios were compared to ^{68}Ga eluates derived from a ^{68}Ge/^{68}Ga-generator (GalliaPharm, Eckert & Ziegler). Compared to the generator-derived ^{68}Ga, the Zn to radioactivity ratio and AMA showed a clear improvement but could not be statistically established due to the small sample quantity.

Compared to ^{68}Ga derived from generators or produced by liquid targets, the solid-target approach has the advantage of significantly higher yields [55]. In this study we simplified the handling of the solid-target preparation by using enriched ^{68}Zn foils and utilised the UTEVA resin to separate the desired ^{68}Ga from other metal ions at optimised concentrations of HCl.

The values of RNP, Zn and Fe corresponded to a shelf-life of the product of 7.7, 12.0 and 6.4 hours from EOB, respectively, with respect to the ^{66}Ga and ^{67}Ga longer half-lives and the metal to activity limits stated in the Eur Pharm Monograph [151]. This made the Fe impurity the limiting factor for the shelf-life of the product.

When considering producing a radionuclide for radiopharmaceutical preparations by a new route, the quality of the obtained radionuclide must be advantageous compared to what is already available. In this case, extra effort is required to produce ^{68}Ga using the cyclotron solid-target system instead of obtaining it from a generator. The AMA estimated in paper III, indicates that radiopharmaceuticals using the DOTA chelator could be produced in higher activities than with generator-derived ^{68}Ga without changing other parameters, such as amounts of the precursor in the synthesis. Amounts of the precursor could be increased so that similar radiosynthesis yields could be achieved, an approach previously reported [59,152] and a tactic commonly used to increase yields in radiochemistry. This is however problematic when the radiopharmaceutical is regulatorily mass limited for injection, e.g. for [^{68}Ga]Ga-DOTATOC [153].

3.4 REFINEMENT OF CYCLOTRON-PRODUCED ^{68}Ga PURIFICATION AND ITS IMPLEMENTATION IN RADIOPHARMACEUTICAL PRODUCTIONS (PAPER IV)

In paper IV the aim was to improve the production of and implement the cyclotron-produced ^{68}Ga eluate for GMP-compliant radiolabelling of clinically relevant DOTA-based radiopharmaceuticals. We aimed for high synthesis out-put, by means of a high radiolabelling yield.

In the initial attempt to produce [^{68}Ga]Ga-DOTATOC using the ^{68}Ga from paper III and 40 µg edotreotide precursor, a yield of ~25% (~2.5 GBq non-corrected product) was obtained. This was, to our knowledge, an improvement compared to previous reports [59,152]. However, with losses of 75% radioactivity, further improvements were desired.

These losses are most likely due to a possible Fe impurity in the production/separation process that was the a limiting factor regarding the shelf-life and especially that the Fe(III) ion is a tough competitor to the Ga(III) ion in the complexation chemistry. Therefore, we developed a refinement of the purification method of the cyclotron solid target produced ^{68}Ga in paper III. The refinement consisted of adding ascorbate to the dilution and wash solutions of the purification. The ascorbate reduces Fe(III) to Fe(II) while Ga(III) is not reduced to Ga(II). Fe(II) was found to have a lower retention to the UTEVA resin and is thereby washed away in the purification process. Ga(III) is retained on the UTEVA. The last step in the purification elutes the Ga(III) to collection, now with decreased amounts of competing Fe. Before implementing this strategy, the hypothesis was confirmed using stable trivalent isotopes, showing a statistically significant decrease in Fe impurity in the ^{68}Ga product when ascorbate was added in the dilution and wash solutions of the purification process. A confirmation of the decrease in amount of Fe was performed by comparing the ^{68}Ga cyclotron eluates produced with and without ascorbate. The final eluates were analysed by ICP-MS and the result showed that the Fe content was substantially lowered by the ascorbate treatment in the purification step.

Titrations performed showed a clear improvement when ascorbate was added to the purification process. See Figure 22. The chelators NOTA and HBED were also included in this study. AMA values for the chelators DOTA, NOTA and HBED were estimated to be 491 ± 204 GBq/µmol, 993 ± 405 GBq/µmol, and 4480 ± 3060 GBq/µmol, respectively.

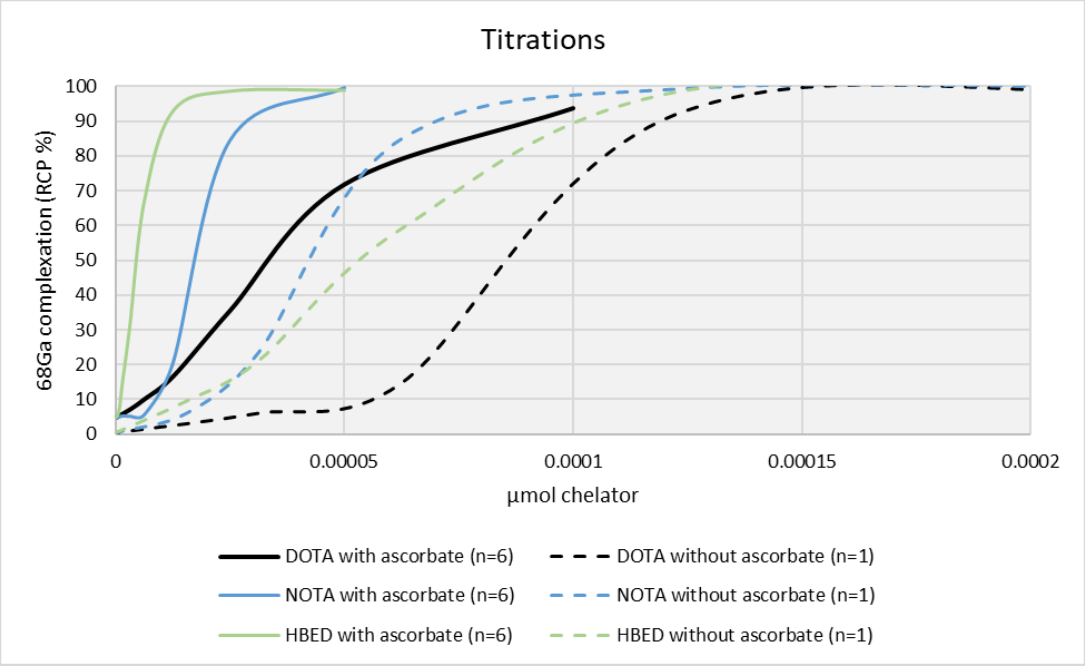

Figure 22. Comparison between titrations with or without ascorbate added in the ^{68}Ga purification process. Figure modified from paper IV.

With the ascorbate added in the purification of the solid-target cyclotron-produced ^{68}Ga, the next step was to use it in radiopharmaceutical productions. The same radiosynthesis methods were used as previously used at the Karolinska University Hospital with generator-derived ^{68}Ga for [^{68}Ga]Ga-DOTATOC and for the FAP inhibitor (FAPI), [^{68}Ga]Ga-FAPI-46, without modifications. The syntheses were performed on an Eckert & Ziegler ModularLab synthesis unit. See results in Table 5.

Table 5. Comparison between syntheses of [^{68}Ga]Ga-FAPI-46 and [^{68}Ga]Ga-DOTATOC made from either generator-derived or solid-target cyclotron-produced ^{68}Ga in paper IV.

	[^{68}Ga]Ga-FAPI-46		**[^{68}Ga]Ga-DOTATOC**	
	Generator (n = 4)	**Cyclotron** (n = 3)	**Generator** (n = 86)	**Cyclotron** (n = 3)
Peptide precursor mass (µg)	50	50	40	40
Product activity (GBq)	0.6 ± 0.1	**5.6** ± 0.3	0.6 ± 0.2	**6.1** ± 1.0
RCY non-corrected (%)	58 ± 3	57 ± 2	61 ± 8	64 ± 4
AMA (GBq/µmol)	10 ± 2	98.8 ± 5.1	21.7 ± 5.6	215.1 ± 36.6

The products met all specifications according to GMP and the relevant Eur Pharm Monographs [151,153] and were stable at least 5 hours after end of synthesis. Stability was analysed with respect to RNP, metal (Zn and Fe) to radioactivity ratios, precursor amount per patient dose and RCP.

Lowering the amount of Fe(III) is crucial for high radiolabelling yields, because Fe(III) will out-compete Ga(III) in the labelling, and this is due to its high log stability constant (log K_{ML}) with, for example, the DOTA chelator [154].

We also wanted to use as little mass of precursor as possible in the syntheses in order to obtain a high AMA. We used the same amount of precursor as for generator-derived ^{68}Ga, and found that we could produce ~10 times more [^{68}Ga]Ga-DOTATOC and [^{68}Ga]Ga-FAPI-46 using our solid-target cyclotron-produced ^{68}Ga.

In conclusion we produced about 6 GBq radiopharmaceutical product from a starting activity of 10 GBq. This means around 20 patient doses instead of the 2 typically obtained when using a ^{68}Ge/^{68}Ga-generator. Titrations with NOTA and HBED chelators indicate an even larger benefit from the ascorbate addition.

4 CONCLUDING REMARKS AND FUTURE PERSPECTIVES

In this thesis two positron-emitting radiometals have been produced by several routes and their distinctive characteristics and labelling behaviours have been exploited in radiochemistry and radionuclide-based molecular imaging studies.

In **paper I** generator-derived ^{68}Ga was used to radiolabel an albumin targeting Affibody molecule. [^{68}Ga]Ga-ABY-028 was evaluated regarding its potential as an *in situ* albumin targeting probe. The albumin targeting capability was confirmed by *in vitro* binding studies and *in vivo* by studies of biodistribution using a small animal PET camera. We propose this novel radiotracer is an excellent tool for studies of vascular permeability to albumin and similarly sized molecules and potentially as a baseline control for non-specific uptake of other ABD-based diagnostic or therapeutic agents. The latter would be highly interesting for evaluations of specific targeting, since uptake of the radiolabelled ABD itself, i.e. [^{68}Ga]Ga-ABY-028, in various tumours was clearly shown in present study. For potential future clinical studies, an automated radiolabelling method should be developed to meet the regulatory quality requirements for GMP-production.

In **paper II** cyclotron-produced ^{89}Zr was used, the radiosyntheses of two different ^{89}Zr-complexes, [^{89}Zr]Zr-(oxine)$_4$ and [^{89}Zr]Zr-DFO-NCS, were optimised and they were compared in a head-to-head cell labelling study. The optimisations resulted in relatively easy radiosynthesis protocols that avoid cumbersome purification steps with minimal radioactive exposure for the operator. Radiolabelling of different cells types showed that both ^{89}Zr-complexes have potential uses for clinical applications, with [^{89}Zr]Zr-(oxine)$_4$ preferred due to its longer shelf-life (between radiosynthesis and use in cell labelling) and its non-discriminating retention between the cell types. The [^{89}Zr]Zr-DFO-NCS approach is still of interest due to the ease of its cell labelling, but improved storage conditions are needed, preventing the fast hydrolysation of the NCS group that likely limits its shelf-life.

In **paper III,** a cyclotron solid target production and purification method was developed to meet the generally increasing demand for ^{68}Ga. In **paper IV**, the purification method was refined to effectively remove the chelating competitive Fe(III). The cyclotron-produced radionuclide obtained was subsequently validated by its use in the labelling of clinically relevant radiopharmaceuticals. With these two studies we have made the use of cyclotron solid target produced ^{68}Ga feasible for labelling DOTA-based radiotracers, with yields and AMA values superior to those using generator-derived ^{68}Ga. To translate the solid target produced radionuclide to clinical radiopharmaceutical productions some regulatory hurdles must be overcome since the radionuclide is currently affected by the fact ^{68}Ge/^{68}Ga generators are themselves registered as radiopharmaceuticals. The cyclotron solid target produced ^{68}Ga should have a bright future for PET facilities with an in-house cyclotron, once it can be included in clinical production settings.

The strategy of coordinating radiometals to biomolecules that bind to specific targets is of increasing interest in the field of molecular imaging as well as for its possible theranostic applications. In this thesis labelling with two of the most common positron-emitting radiometals, ^{68}Ga and ^{89}Zr, was explored. The choices of radionuclides were made with regards to their suitable half-lives, but also because of their availability. The strategies and approaches examined here have potential for translation to more exotic radiometals in the future, to potentially expand the palette of chemical properties that can be used in radiolabelling, as well as the decay characteristics and time-windows for imaging. Since the cyclotron solid target approach allows for production of a wide variety of radiometals and methods and techniques for radiometal labelling explored in this thesis allows for translation to other specific tissue targeting molecules or cells, this journey has just begun.

5 ACKNOWLEDGEMENTS

I want to express my deepest gratitude to everyone who has contributed to this thesis, other adjacent research projects or simply been there for me during my doctoral studies – my benefactors.

The Governmental Agency for Innovation Systems (Vinnova), the Swedish Cancer Society, the Söderberg Foundation, the Swedish Research Council, the Cancer Research Funds of Radiumhemmet and the King Gustaf V Jubilee Fund, the Karolinska Institutet, and the Karolinska University Hospital are acknowledged for financing.

First of all, **Thuy Tran**, my main supervisor. Thank you for your terrific scientific guidance and for challenging me in a well-balanced way. You have made me believe in my own potential. Thank you for being my friend and research partner. Your enthusiasm and curiosity are truly contagious!

Sharon Stone-Elander, my co-supervisor, my first main supervisor. I am so happy and grateful you opened the door to science for me. Always generous, whether it's science or life in general that is the subject for our conversation. You have an awesome laugh and are such a warm person.

Erik Samén, my co-supervisor. You guided me through the first ever radiosynthesis I made back in the ancient times. It feels safe to have you, my oldest colleague, still by my side (or a little above – boss).

Staffan Holmin, my co-supervisor. Thank you for welcoming us radiochemists/pharmacists into your research group and for financial support during my first years as a graduate student.

Cathrine Jonsson, my mentor. Always supporting and easy to talk to. Thank you incredibly much for providing me a calm place for writing this thesis (which may have been crucial).

Many warm thanks to my present research group, the **TRANslational Radiotheranostics** group. You are all fantastic and great to work with! There are some exciting years ahead to look forward to. Who knows what we will be able to accomplish?!

Jonathan Siikanen and **Stefan Milton**, spjutspetsforskarna. It has been sooo much fun working with you in the solid target project. No ending here. You are both funny crazy, but genius.

Ida Friberger, thank you for the collaboration on ^{89}Zr-labelling and for your skills with cells. Also, thank you to **Jeroen Goos** for ditto reason.

I am grateful for good and helpful administration by **Erika Rindsjö** (at Oncology and Pathology) and **Anna Prave Hedestedt** (at Karolinska Radiopharmacy).

Director of doctoral studies **Andreas Lundqvist** and head of department **Lars Holmgren.** Thank you for your support and good advises along the way.

To all **co-authors** and **collaborators** that have contributed to the papers included in this thesis, and adjacent papers accepted over the years. You have undoubtfully enriched my vision and taught me a lot.

The Department of Medical Radiation Physics and Nuclear Medicine (especially **Rimma Axelsson** and **Alejandro Sanchez Crespo**) for great clinical and research collaborations over the years. Also, a special thank you to the **Huddinge site** for your warm welcoming and for providing me interesting lunch discussions during my thesis writing period.

Jan-Olov Thorell, J-O, Thor-El, the true head-of-production, at least in my mind. I really enjoyed working inside and outside of the lab with you, no fuss. Christina: the raggsockor are still going strong. I wear them right now btw.

No animal experiments included in this thesis would have been possible without you, wonderful **Li Lu**. You have such skills. I'm amazed. You tried to teach me Chinese at some point, but I have to admit, I am a hopeless case.

Lovely **Tetyana Tegnebratt**, Tanya, the kindest person ever. Thank you for the collaboration with the ABY-028 paper and for just being you. You and maybe Li and Sharon may continue calling me "lilla gumman" without me getting fierce feelings going. :-) It's ok.

Jonas Grafström, thank you for making my first year as a graduate student a little goofier, for the small cups of delicious coffee and for teaching me how to draw a ROI.

Thanks to the Holmin group members, especially **Fabian Arnberg**, **Johan Lundberg**, **Philip Little** and **Arvin Chireh** for good collaboration and for your expertise with catheters and wires.

My former office buddy, **Henrik Alfredéen**, "the king" of radiopharmacy (sure). You are fun. Now let's develop the … out of every radiotracer requested together!

Thank you, **Carsten Steiger**, for taking the quality system of the radiopharmacy to the level we use today. Without your mindset I think it would have been hard to meet and concur many of the obstacles related to pharmaceutical production. Also, thank you for being a good friend.

To everyone at **the Karolinska Radiopharmacy**: **Anna-Karin, Azad, Azadeh, Denice, Ellen, Elionore, Fredrik, Hanna E, Hanna O, Karolina, Kevin, Lovisa, Marléne, Matthias, Mohammad, Mélodie, Nancy, Paul, Petra, Rasta, Seth** and **Valda**. You all have contributed to this thesis in one or another way, directly or even if you declare yourself unaware of it. You brighten my days at Karolinska!

To all my former workmates (especially **Kenneth, Rebecka**, **Johanna**, **Patrick**, **Anne** and **Madjid)**, you are fantastic and thank you for crucial support and for covering up for me during experiments of my graduate studies.

Marco Lopes, the Karolinska GE Healthcare engineer, thank you for your hard work with keeping the cyclotrons and most of the other equipment at the radiopharmacy facility going.

To all personnel from the **KI-psychiatry** and **Astra Zeneca** groups. Thank you for a smooth collaboration in the PET labs, both at the old and the new site. A special thank you to **Johan Ulin** who first introduced me to ^{68}Ga-chemistry.

Inte tack till mitt **vänsterknä** som inte vill samarbeta efter skada och operationer. Däremot, tack till fysioterapeut **Joel** som stöttat och peppat under många timmar av rehab.

Tack fina **pappa** för att du alltid stöttat och hejat på mig i vad jag än tagit mig för. Tack också till mina coola stora brorsor, **Mats** och **Tobbe**. Jag skickar iväg ett varmt tack till **mamma** och **Tomas** också såklart, jag önskar att ni fortfarande fanns med oss. Ni betyder mycket för mig.

Ulla och **Uffe**, mina svärföräldrar, mina extraföräldrar. Tack för att ni finns, stöttar och peppar.

Till min fru **Åsa,** tack för att du har visat förståelse och dragit det lite tyngre lasset när det har behövts, speciellt vid skrivandet av denna avhandling. Tack till våra fina barn, **Vidar** och **Algot**, för att ni påminner om vad som är viktigast. *Jag älskar er.* ♥

6 REFERENCES

1. Massoud, T.F.; Gambhir, S.S. Molecular imaging in living subjects: seeing fundamental biological processes in a new light. *Genes Dev* 2003, *17*, 545-580, doi:10.1101/gad.1047403.

2. Rowe, S.P.; Pomper, M.G. Molecular imaging in oncology: Current impact and future directions. *CA Cancer J Clin* 2021, doi:10.3322/caac.21713.

3. Bartholomä, M.D. Recent developments in the design of bifunctional chelators for metal-based radiopharmaceuticals used in Positron Emission Tomography. *Inorganica Chimica Acta* 2012, *389*, 36-51, doi:https://doi.org/10.1016/j.ica.2012.01.061.

4. Wadsak, W.; Mitterhauser, M. Basics and principles of radiopharmaceuticals for PET/CT. *Eur J Radiol* 2010, *73*, 461-469, doi:10.1016/j.ejrad.2009.12.022.

5. Jeong, J.M. The Importance of Radiopharmaceutical Chemistry for the Development of Nuclear Medicine: a Message from the Associate Editor. *Nucl Med Mol Imaging* 2015, *49*, 169, doi:10.1007/s13139-015-0355-z.

6. Jackson, J.; Hungnes, I.; Ma, M.T.; Rivas, C. Bioconjugates of Chelators with Peptides and Proteins in Nuclear Medicine: Historical Importance, Current Innovations and Future Challenges. *Bioconjug Chem* 2020, doi:10.1021/acs.bioconjchem.0c00015.

7. Bansal, A.; Pandey, M.K.; Demirhan, Y.E.; Nesbitt, J.J.; Crespo-Diaz, R.J.; Terzic, A.; Behfar, A.; DeGrado, T.R. Novel ^{89}Zr cell labeling approach for PET-based cell trafficking studies. *EJNMMI Res* 2015, *5*, 19, doi:10.1186/s13550-015-0098-y.

8. Kocarnik, J.M.; Compton, K.; Dean, F.E.; Fu, W.; Gaw, B.L.; Harvey, J.D.; Henrikson, H.J.; Lu, D.; Pennini, A.; Xu, R.; et al. Cancer Incidence, Mortality, Years of Life Lost, Years Lived With Disability, and Disability-Adjusted Life Years for 29 Cancer Groups From 2010 to 2019: A Systematic Analysis for the Global Burden of Disease Study 2019. *JAMA Oncol* 2021, doi:10.1001/jamaoncol.2021.6987.

9. Hanahan, D.; Weinberg, R.A. The hallmarks of cancer. *Cell* 2000, *100*, 57-70, doi:10.1016/s0092-8674(00)81683-9.

10. Hanahan, D.; Weinberg, Robert A. Hallmarks of Cancer: The Next Generation. *Cell* 2011, *144*, 646-674, doi:https://doi.org/10.1016/j.cell.2011.02.013.

11. Ge, S.; Li, J.; Yu, Y.; Chen, Z.; Yang, Y.; Zhu, L.; Sang, S.; Deng, S. Review: Radionuclide Molecular Imaging Targeting HER2 in Breast Cancer with a Focus on Molecular Probes into Clinical Trials and Small Peptides. *Molecules* 2021, *26*, doi:10.3390/molecules26216482.

12. Giraudet, A.-L.; Kryza, D.; Hofman, M.; Moreau, A.; Fizazi, K.; Flechon, A.; Hicks, R.J.; Tran, B. PSMA targeting in metastatic castration-resistant prostate cancer: where are we and where are we going? *Therapeutic Advances in Medical Oncology* 2021, *13*, 17588359211053898, doi:10.1177/17588359211053898.

13. Taboada, G.F.; Luque, R.M.; Neto, L.V.; Machado, E.d.O.; Sbaffi, B.C.; Domingues, R.C.; Marcondes, J.B.; Chimelli, L.M.C.; Fontes, R.; Niemeyer, P.; et al. Quantitative analysis of somatostatin receptor subtypes (1–5) gene expression levels in

somatotropinomas and correlation to in vivo hormonal and tumor volume responses to treatment with octreotide LAR. *European Journal of Endocrinology* 2008, *158*, 295-303, doi:10.1530/EJE-07-0562.

14. Nader-Marta, G.; Martins-Branco, D.; de Azambuja, E. How we treat patients with metastatic HER2-positive breast cancer. *ESMO Open* 2022, *7*, 100343, doi:https://doi.org/10.1016/j.esmoop.2021.100343.

15. Kratochwil, C.; Giesel, F.L.; Stefanova, M.; Benešová, M.; Bronzel, M.; Afshar-Oromieh, A.; Mier, W.; Eder, M.; Kopka, K.; Haberkorn, U. PSMA-Targeted Radionuclide Therapy of Metastatic Castration-Resistant Prostate Cancer with ^{177}Lu-Labeled PSMA-617. *J Nucl Med* 2016, *57*, 1170-1176, doi:10.2967/jnumed.115.171397.

16. Atkinson, C.; Ganeshan, B.; Endozo, R.; Wan, S.; Aldridge, M.D.; Groves, A.M.; Bomanji, J.B.; Gaze, M.N. Radiomics-Based Texture Analysis of ^{68}Ga-DOTATATE Positron Emission Tomography and Computed Tomography Images as a Prognostic Biomarker in Adults With Neuroendocrine Cancers Treated With ^{177}Lu-DOTATATE. *Front Oncol* 2021, *11*, 686235, doi:10.3389/fonc.2021.686235.

17. Hennrich, U.; Benešová, M. [^{68}Ga]Ga-DOTA-TOC: The First FDA-Approved ^{68}Ga-Radiopharmaceutical for PET Imaging. *Pharmaceuticals (Basel)* 2020, *13*, doi:10.3390/ph13030038.

18. Eapen, R.S.; Nzenza, T.C.; Murphy, D.G.; Hofman, M.S.; Cooperberg, M.; Lawrentschuk, N. PSMA PET applications in the prostate cancer journey: from diagnosis to theranostics. *World Journal of Urology* 2019, *37*, 1255-1261, doi:10.1007/s00345-018-2524-z.

19. Velikyan, I.; Schweighöfer, P.; Feldwisch, J.; Seemann, J.; Frejd, F.Y.; Lindman, H.; Sörensen, J. Diagnostic HER2-binding radiopharmaceutical, [^{68}Ga]Ga-ABY-025, for routine clinical use in breast cancer patients. *Am J Nucl Med Mol Imaging* 2019, *9*, 12-23.

20. Gullberg, G.T.; Reutter, B.W.; Sitek, A.; Maltz, J.S.; Budinger, T.F. Dynamic single photon emission computed tomography--basic principles and cardiac applications. *Phys Med Biol* 2010, *55*, R111-191, doi:10.1088/0031-9155/55/20/R01.

21. Townsend, D.W. Physical principles and technology of clinical PET imaging. *Ann Acad Med Singap* 2004, *33*, 133-145.

22. Hungnes, I.N.; Al-Salemee, F.; Gawne, P.J.; Eykyn, T.; Atkinson, R.A.; Terry, S.Y.A.; Clarke, F.; Blower, P.J.; Pringle, P.G.; Ma, M.T. One-step, kit-based radiopharmaceuticals for molecular SPECT imaging: a versatile diphosphine chelator for ^{99m}Tc radiolabelling of peptides. *Dalton Trans* 2021, *50*, 16156-16165, doi:10.1039/d1dt03177e.

23. Sanchez-Crespo, A.; Andreo, P.; Larsson, S.A. Positron flight in human tissues and its influence on PET image spatial resolution. *Eur J Nucl Med Mol Imaging* 2004, *31*, 44-51, doi:10.1007/s00259-003-1330-y.

24. Lundqvist, H.; Tolmachev, V. Targeting peptides and positron emission tomography. *Biopolymers* 2002, *66*, 381-392, doi:10.1002/bip.10348.

25. Sanchez-Crespo, A. Comparison of Gallium-68 and Fluorine-18 imaging characteristics in positron emission tomography. *Applied Radiation and Isotopes* 2013, *76*, 55-62, doi:https://doi.org/10.1016/j.apradiso.2012.06.034.

26. Spick, C.; Herrmann, K.; Czernin, J. ^{18}F-FDG PET/CT and PET/MRI Perform Equally Well in Cancer: Evidence from Studies on More Than 2,300 Patients. *Journal of Nuclear Medicine* 2016, *57*, 420, doi:10.2967/jnumed.115.158808.

27. Seifert, R.; Kersting, D.; Rischpler, C.; Opitz, M.; Kirchner, J.; Pabst, K.M.; Mavroeidi, I.A.; Laschinsky, C.; Grueneisen, J.; Schaarschmidt, B.; et al. Clinical Use of PET/MR in Oncology: An Update. *Semin Nucl Med* 2021, doi:10.1053/j.semnuclmed.2021.11.012.

28. Yang, C.-T.; Ghosh, K.K.; Padmanabhan, P.; Langer, O.; Liu, J.; Eng, D.N.C.; Halldin, C.; Gulyás, B. PET-MR and SPECT-MR multimodality probes: Development and challenges. *Theranostics* 2018, *8*, 6210-6232, doi:10.7150/thno.26610.

29. Johnstrom, P.; Bird, J.L.; Davenport, A.P. Quantitative phosphor imaging autoradiography of radioligands for positron emission tomography. *Methods Mol Biol* 2012, *897*, 205-220, doi:10.1007/978-1-61779-909-9_10.

30. Green, M.R.; Sambrook, J. Autoradiography and Phosphorimaging. *Cold Spring Harbor protocols* 2020, *2020*, pdb.top100446, doi:10.1101/pdb.top100446.

31. Cutler, C.S.; Hennkens, H.M.; Sisay, N.; Huclier-Markai, S.; Jurisson, S.S. Radiometals for combined imaging and therapy. *Chem Rev* 2013, *113*, 858-883, doi:10.1021/cr3003104.

32. Notni, J.; Wester, H.J. Re-thinking the role of radiometal isotopes: Towards a future concept for theranostic radiopharmaceuticals. *J Labelled Comp Radiopharm* 2018, *61*, 141-153, doi:10.1002/jlcr.3582.

33. Sofou, S. Radionuclide carriers for targeting of cancer. *Int J Nanomedicine* 2008, *3*, 181-199, doi:10.2147/ijn.s2736.

34. Zeglis, B.M.; Lewis, J.S. A practical guide to the construction of radiometallated bioconjugates for positron emission tomography. *Dalton Trans* 2011, *40*, 6168-6195, doi:10.1039/c0dt01595d.

35. Fersing, C.; Bouhlel, A.; Cantelli, C.; Garrigue, P.; Lisowski, V.; Guillet, B. A Comprehensive Review of Non-Covalent Radiofluorination Approaches Using Aluminum [^{18}F]fluoride: Will [^{18}F]AlF Replace ^{68}Ga for Metal Chelate Labeling? *Molecules* 2019, *24*, doi:10.3390/molecules24162866.

36. Blower, J.E.; Cooper, M.S.; Imberti, C.; Ma, M.T.; Marshall, C.; Young, J.D.; Blower, P.J. The Radiopharmaceutical Chemistry of the Radionuclides of Gallium and Indium. In *Radiopharmaceutical Chemistry*, Lewis, J.S., Windhorst, A.D., Zeglis, B.M., Eds.; Springer, Cham: 2019; Volume 1.

37. Bartholomä, M.D.; Louie, A.S.; Valliant, J.F.; Zubieta, J. Technetium and gallium derived radiopharmaceuticals: comparing and contrasting the chemistry of two important radiometals for the molecular imaging era. *Chem Rev* 2010, *110*, 2903-2920, doi:10.1021/cr1000755.

38. Banerjee, S.R.; Pomper, M.G. Clinical applications of Gallium-68. *Applied radiation and isotopes : including data, instrumentation and methods for use in agriculture, industry and medicine* 2013, *76*, 2-13, doi:10.1016/j.apradiso.2013.01.039.

39. Fani, M.; André, J.P.; Maecke, H.R. ^{68}Ga-PET: a powerful generator-based alternative to cyclotron-based PET radiopharmaceuticals. *Contrast Media Mol Imaging* 2008, *3*, 67-77, doi:10.1002/cmmi.232.

40. Brandt, M.; Cardinale, J.; Aulsebrook, M.L.; Gasser, G.; Mindt, T.L. An Overview of PET Radiochemistry, Part 2: Radiometals. *J Nucl Med* 2018, *59*, 1500-1506, doi:10.2967/jnumed.117.190801.

41. Heskamp, S.; Raavé, R.; Boerman, O.; Rijpkema, M.; Goncalves, V.; Denat, F. ^{89}Zr-Immuno-Positron Emission Tomography in Oncology: State-of-the-Art ^{89}Zr Radiochemistry. *Bioconjug Chem* 2017, *28*, 2211-2223, doi:10.1021/acs.bioconjchem.7b00325.

42. Alzimami, K.S.; Ma, A.K. Effective dose to staff members in a positron emission tomography/CT facility using zirconium-89. *Br J Radiol* 2013, *86*, 20130318, doi:10.1259/bjr.20130318.

43. Wadas, T.J.; Wong, E.H.; Weisman, G.R.; Anderson, C.J. Coordinating radiometals of copper, gallium, indium, yttrium, and zirconium for PET and SPECT imaging of disease. *Chem Rev* 2010, *110*, 2858-2902, doi:10.1021/cr900325h.

44. Vugts, D.J.; van Dongen, G.A.M.S. ^{89}Zr-labeled compounds for PET imaging guided personalized therapy. *Drug Discovery Today: Technologies* 2011, *8*, e53-e61, doi:https://doi.org/10.1016/j.ddtec.2011.12.004.

45. Kurebayashi, Y.; Choyke, P.L.; Sato, N. Imaging of cell-based therapy using ^{89}Zr-oxine ex vivo cell labeling for positron emission tomography. *Nanotheranostics* 2021, *5*, 27-35, doi:10.7150/ntno.51391.

46. ClinicalTrials.gov Identifier: NCT03807973 Tracking Peripheral Immune Cell Infiltration of the Brain in Central Inflammatory Disorders Using [Zr-89]Oxinate-4-labeled Leukocytes (accessed on February 21, 2022).

47. Zhou, Y.; Li, J.; Xu, X.; Zhao, M.; Zhang, B.; Deng, S.; Wu, Y. ^{64}Cu-based Radiopharmaceuticals in Molecular Imaging. *Technology in cancer research & treatment* 2019, *18*, 1533033819830758-1533033819830758, doi:10.1177/1533033819830758.

48. Peres, E.A.; Toutain, J.; Paty, L.P.; Divoux, D.; Ibazizene, M.; Guillouet, S.; Barre, L.; Vidal, A.; Cherel, M.; Bourgeois, M.; et al. ^{64}Cu-ATSM/^{64}Cu-Cl_2 and their relationship to hypoxia in glioblastoma: a preclinical study. *EJNMMI Res* 2019, *9*, 114, doi:10.1186/s13550-019-0586-6.

49. Chatal, J.F.; Rouzet, F.; Haddad, F.; Bourdeau, C.; Mathieu, C.; Le Guludec, D. Story of Rubidium-82 and Advantages for Myocardial Perfusion PET Imaging. *Front Med (Lausanne)* 2015, *2*, 65, doi:10.3389/fmed.2015.00065.

50. Pillai, M.R.A.; Dash, A.; Knapp, F.F. Sustained Availability of ^{99m}Tc: Possible Paths Forward. *Journal of Nuclear Medicine* 2013, *54*, 313, doi:10.2967/jnumed.112.110338.

51. Dash, A.; Chakravarty, R. Radionuclide generators: the prospect of availing PET radiotracers to meet current clinical needs and future research demands. *American journal of nuclear medicine and molecular imaging* 2019, *9*, 30-66.

52. Rösch, F. Past, present and future of ^{68}Ge/^{68}Ga generators. *Appl Radiat Isot* 2013, *76*, 24-30, doi:10.1016/j.apradiso.2012.10.012.

53. IAEA. Cyclotron Produced Radionuclides: Principles and Practice. Technical report series no.465. International Atomic Energy Agency: 2008.

54. Pichler, V.; Berroteran-Infante, N.; Philippe, C.; Vraka, C.; Klebermass, E.M.; Balber, T.; Pfaff, S.; Nics, L.; Mitterhauser, M.; Wadsak, W. An Overview of PET Radiochemistry, Part 1: The Covalent Labels ^{18}F, ^{11}C, and ^{13}N. *J Nucl Med* 2018, *59*, 1350-1354, doi:10.2967/jnumed.117.190793.

55. IAEA. Gallium-68 Cyclotron Production IAEA-TECDOC-1863. International Atomic Energy Agency: 2019.

56. Pandey, M.K.; DeGrado, T.R. Cyclotron Production of PET Radiometals in Liquid Targets: Aspects and Prospects. *Curr Radiopharm* 2020, doi:10.2174/1874471013999200820165734.

57. Pandey, M.K.; Byrne, J.F.; Jiang, H.; Packard, A.B.; DeGrado, T.R. Cyclotron production of ^{68}Ga via the ^{68}Zn(p,n)^{68}Ga reaction in aqueous solution. *Am J Nucl Med Mol Imaging* 2014, *4*, 303-310.

58. Lin, M.; Waligorski, G.J.; Lepera, C.G. Production of curie quantities of ^{68}Ga with a medical cyclotron via the ^{68}Zn(p,n)^{68}Ga reaction. *Appl Radiat Isot* 2018, *133*, 1-3, doi:10.1016/j.apradiso.2017.12.010.

59. Tieu, W.; Hollis, C.A.; Kuan, K.K.W.; Takhar, P.; Stuckings, M.; Spooner, N.; Malinconico, M. Rapid and automated production of [^{68}Ga]gallium chloride and [^{68}Ga]Ga-DOTA-TATE on a medical cyclotron. *Nucl Med Biol* 2019, *74-75*, 12-18, doi:10.1016/j.nucmedbio.2019.07.005.

60. Svedjehed, J.; Pärnaste, M.; Gagnon, K. Demystifying solid targets: Simple and rapid distribution-scale production of [^{68}Ga]$GaCl_3$ and [^{68}Ga]Ga-PSMA-11. *Nucl Med Biol* 2021, *104-105*, 1-10, doi:10.1016/j.nucmedbio.2021.10.002.

61. Alnahwi, A.H.; Tremblay, S.; Ait-Mohand, S.; Beaudoin, J.F.; Guérin, B. Automated radiosynthesis of ^{68}Ga for large-scale routine production using ^{68}Zn pressed target. *Appl Radiat Isot* 2020, *156*, 109014, doi:10.1016/j.apradiso.2019.109014.

62. Zeisler, S.; Limoges, A.; Kumlin, J.; Siikanen, J.; Hoehr, C. Fused Zinc Target for the Production of Gallium Radioisotopes. *Instruments* 2019, *3*, 10.

63. Skliarova, H.; Cisternino, S.; Cicoria, G.; Marengo, M.; Cazzola, E.; Gorgoni, G.; Palmieri, V. Medical Cyclotron Solid Target Preparation by Ultrathick Film Magnetron Sputtering Deposition. *Instruments* 2019, *3*, 21.

64. Holland, J.P.; Sheh, Y.; Lewis, J.S. Standardized methods for the production of high specific-activity zirconium-89. *Nucl Med Biol* 2009, *36*, 729-739, doi:10.1016/j.nucmedbio.2009.05.007.

65. Severin, G.W.; Engle, J.W.; Barnhart, T.E.; Nickles, R.J. ^{89}Zr radiochemistry for positron emission tomography. *Med Chem* 2011, *7*, 389-394, doi:10.2174/157340611796799186.

66. IAEA-NDS. Charged-particle Cross Section Database for Medical Radioisotope Production and Beam Monitor Reactions. Available online: https://www-nds.iaea.org/medical/index.html (accessed on Feb. 8).

67. Martiniova, L.; Palatis, L.; Etchebehere, E.; Ravizzini, G. Gallium-68 in Medical Imaging. *Curr Radiopharm* 2016, *9*, 187-207, doi:10.2174/1874471009666161028150654.

68. Toyota, T.; Hanafusa, T.; Oda, T.; Koumura, I.; Sasaki, T.; Matsuura, E.; Kumon, H.; Yano, T.; Ono, T. A purification system for ^{64}Cu produced by a biomedical cyclotron

for antibody PET imaging. *J Radioanal Nucl Chem* 2013, *298*, 295-300, doi:10.1007/s10967-012-2340-7.

69. Coenen, H.H.; Gee, A.D.; Adam, M.; Antoni, G.; Cutler, C.S.; Fujibayashi, Y.; Jeong, J.M.; Mach, R.H.; Mindt, T.L.; Pike, V.W.; et al. Consensus nomenclature rules for radiopharmaceutical chemistry — Setting the record straight. *Nuclear Medicine and Biology* 2017, *55*, v-xi, doi:https://doi.org/10.1016/j.nucmedbio.2017.09.004.

70. Kostelnik, T.I.; Orvig, C. Radioactive Main Group and Rare Earth Metals for Imaging and Therapy. *Chem Rev* 2019, *119*, 902-956, doi:10.1021/acs.chemrev.8b00294.

71. Larenkov, A.; Bubenschikov, V.; Makichyan, A.; Zhukova, M.; Krasnoperova, A.; Kodina, G. Preparation of Zirconium-89 Solutions for Radiopharmaceutical Purposes: Interrelation Between Formulation, Radiochemical Purity, Stability and Biodistribution. *Molecules* 2019, *24*, doi:10.3390/molecules24081534.

72. Mueller, D.; Klette, I.; Baum, R.P. Purification and Labeling Strategies for ^{68}Ga from ^{68}Ge/^{68}Ga Generator Eluate. In Proceedings of the Theranostics, Gallium-68, and Other Radionuclides, Berlin, Heidelberg, 2013//, 2013; pp. 77-87.

73. Velikyan, I.; Beyer, G.J.; Langstrom, B. Microwave-supported preparation of ^{68}Ga bioconjugates with high specific radioactivity. *Bioconjug Chem* 2004, *15*, 554-560, doi:10.1021/bc030078f.

74. Bauwens, M.; Chekol, R.; Vanbilloen, H.; Bormans, G.; Verbruggen, A. Optimal buffer choice of the radiosynthesis of ^{68}Ga-Dotatoc for clinical application. *Nucl Med Commun* 2010, *31*, 753-758, doi:10.1097/MNM.0b013e32833acb99.

75. Eppard, E.; Pèrez-Malo, M.; Rösch, F. Improved radiolabeling of DOTATOC with trivalent radiometals for clinical application by addition of ethanol. *EJNMMI Radiopharm Chem* 2017, *1*, 6, doi:10.1186/s41181-016-0010-8.

76. Asti, M.; Iori, M.; Capponi, P.C.; Rubagotti, S.; Fraternali, A.; Versari, A. Development of a simple kit-based method for preparation of pharmaceutical-grade ^{68}Ga-DOTATOC. *Nuclear Medicine Communications* 2015, *36*.

77. Naka, S.; Watabe, T.; Lindner, T.; Cardinale, J.; Kurimoto, K.; Moore, M.; Tatsumi, M.; Mori, Y.; Shimosegawa, E.; Valla, F., Jr.; et al. One-pot and one-step automated radio-synthesis of [^{18}F]AlF-FAPI-74 using a multi purpose synthesizer: a proof-of-concept experiment. *EJNMMI Radiopharm Chem* 2021, *6*, 28, doi:10.1186/s41181-021-00142-z.

78. Zhang, Y.; Hong, H.; Cai, W. PET tracers based on Zirconium-89. *Current radiopharmaceuticals* 2011, *4*, 131-139, doi:10.2174/1874471011104020131.

79. Das, S.S.; Chattopadhyay, S.; Barua, L.; Das, M.K. Production of ^{61}Cu using natural cobalt target and its separation using ascorbic acid and common anion exchange resin. *Applied Radiation and Isotopes* 2012, *70*, 365-368, doi:https://doi.org/10.1016/j.apradiso.2011.10.011.

80. Velikyan, I.; Wennborg, A.; Feldwisch, J.; Lindman, H.; Carlsson, J.; Sörensen, J. Good manufacturing practice production of [^{68}Ga]Ga-ABY-025 for HER2 specific breast cancer imaging. *Am J Nucl Med Mol Imaging* 2016, *6*, 135-153.

81. Kleynhans, J.; Rubow, S.; le Roux, J.; Marjanovic-Painter, B.; Zeevaart, J.R.; Ebenhan, T. Production of [^{68}Ga]Ga-PSMA: Comparing a manual kit-based method with a module-based automated synthesis approach. *Journal of Labelled Compounds and Radiopharmaceuticals* 2020, *63*, 553-563, doi:https://doi.org/10.1002/jlcr.3879.

82. Mellor, D.P. CHAPTER 1 - Historical Background and Fundamental Concepts. In *Chelating Agents and Metal Chelates*, Dwyer, F.P., Mellor, D.P., Eds.; Academic Press: 1964; pp. 1-50.

83. Structures of Metal Complexes [Internet]. 2020 [cited 2022 Jan 24]. Available from: https://chem.libretexts.org/@go/page/125406.

84. Price, E.W.; Orvig, C. Matching chelators to radiometals for radiopharmaceuticals. *Chem Soc Rev* 2014, *43*, 260-290, doi:10.1039/c3cs60304k.

85. De Silva, R.A.; Kumar, D.; Lisok, A.; Chatterjee, S.; Wharram, B.; Venkateswara Rao, K.; Mease, R.; Dannals, R.F.; Pomper, M.G.; Nimmagadda, S. Peptide-Based ^{68}Ga-PET Radiotracer for Imaging PD-L1 Expression in Cancer. *Mol Pharm* 2018, *15*, 3946-3952, doi:10.1021/acs.molpharmaceut.8b00399.

86. Bensch, F.; van der Veen, E.L.; Lub-de Hooge, M.N.; Jorritsma-Smit, A.; Boellaard, R.; Kok, I.C.; Oosting, S.F.; Schroder, C.P.; Hiltermann, T.J.N.; van der Wekken, A.J.; et al. ^{89}Zr-atezolizumab imaging as a non-invasive approach to assess clinical response to PD-L1 blockade in cancer. *Nat Med* 2018, *24*, 1852-1858, doi:10.1038/s41591-018-0255-8.

87. Van Binnebeek, S.; Vanbilloen, B.; Baete, K.; Terwinghe, C.; Koole, M.; Mottaghy, F.M.; Clement, P.M.; Mortelmans, L.; Bogaerts, K.; Haustermans, K.; et al. Comparison of diagnostic accuracy of ^{111}In-pentetreotide SPECT and ^{68}Ga-DOTATOC PET/CT: A lesion-by-lesion analysis in patients with metastatic neuroendocrine tumours. *Eur Radiol* 2016, *26*, 900-909, doi:10.1007/s00330-015-3882-1.

88. McCarthy, M.; Francis, R.; Tang, C.; Watts, J.; Campbell, A. A Multicenter Prospective Clinical Trial of ^{68}Gallium PSMA HBED-CC PET-CT Restaging in Biochemically Relapsed Prostate Carcinoma: Oligometastatic Rate and Distribution Compared With Standard Imaging. *Int J Radiat Oncol Biol Phys* 2019, *104*, 801-808, doi:10.1016/j.ijrobp.2019.03.014.

89. Spang, P.; Herrmann, C.; Roesch, F. Bifunctional Gallium-68 Chelators: Past, Present, and Future. *Semin Nucl Med* 2016, *46*, 373-394, doi:10.1053/j.semnuclmed.2016.04.003.

90. Manoharan, P.; Lamarca, A.; Navalkissoor, S.; Calero, J.; Chan, P.S.; Julyan, P.; Sierra, M.; Caplin, M.; Valle, J. Safety, tolerability and clinical implementation of 'ready-to-use' ^{68}gallium-DOTA0-Tyr3-octreotide (^{68}Ga-DOTATOC) (SomaKIT TOC) for injection in patients diagnosed with gastroenteropancreatic neuroendocrine tumours (GEP-NETs). *ESMO Open* 2020, *5*, doi:10.1136/esmoopen-2019-000650.

91. Calderoni, L.; Farolfi, A.; Pianori, D.; Maietti, E.; Cabitza, V.; Lambertini, A.; Ricci, G.; Telo, S.; Lodi, F.; Castellucci, P.; et al. Evaluation of an Automated Module Synthesis and a Sterile Cold Kit–Based Preparation of ^{68}Ga-PSMA-11 in Patients with Prostate Cancer. *Journal of Nuclear Medicine* 2020, *61*, 716, doi:10.2967/jnumed.119.231605.

92. Feiner, I.V.J.; Brandt, M.; Cowell, J.; Demuth, T.; Vugts, D.; Gasser, G.; Mindt, T.L. The Race for Hydroxamate-Based Zirconium-89 Chelators. *Cancers (Basel)* 2021, *13*, doi:10.3390/cancers13174466.

93. Deng, H.; Wang, H.; Li, Z. Matching Chelators to Radiometals for Positron Emission Tomography Imaging- Guided Targeted Drug Delivery. *Curr Drug Targets* 2015, *16*, 610-624, doi:10.2174/1389450116666150707100702.

94. Tsionou, M.I.; Knapp, C.E.; Foley, C.A.; Munteanu, C.R.; Cakebread, A.; Imberti, C.; Eykyn, T.R.; Young, J.D.; Paterson, B.M.; Blower, P.J.; et al. Comparison of macrocyclic and acyclic chelators for gallium-68 radiolabelling. *RSC Adv* 2017, *7*, 49586-49599, doi:10.1039/c7ra09076e.

95. Holland, J.P. Predicting the Thermodynamic Stability of Zirconium Radiotracers. *Inorg Chem* 2020, doi:10.1021/acs.inorgchem.9b03515.

96. Velikyan, I. ^{68}Ga-Based radiopharmaceuticals: production and application relationship. *Molecules* 2015, *20*, 12913-12943, doi:10.3390/molecules200712913.

97. Pandya, D.N.; Bhatt, N.; Yuan, H.; Day, C.S.; Ehrmann, B.M.; Wright, M.; Bierbach, U.; Wadas, T.J. Zirconium tetraazamacrocycle complexes display extraordinary stability and provide a new strategy for zirconium-89-based radiopharmaceutical development. *Chem Sci* 2017, *8*, 2309-2314, doi:10.1039/c6sc04128k.

98. Dammes, N.; Peer, D. Monoclonal antibody-based molecular imaging strategies and theranostic opportunities. *Theranostics* 2020, *10*, 938-955, doi:10.7150/thno.37443.

99. Pagani, M.; StoneElander, S.; Larsson, S.A. Alternative positron emission tomography with non-conventional positron emitters: effects of their physical properties on image quality and potential clinical applications. *European Journal of Nuclear Medicine* 1997, *24*, 1301-1327, doi:DOI 10.1007/s002590050156.

100. Li, Z.; Li, Y.; Chang, H.P.; Chang, H.Y.; Guo, L.; Shah, D.K. Effect of Size on Solid Tumor Disposition of Protein Therapeutics. *Drug Metab Dispos* 2019, *47*, 1136-1145, doi:10.1124/dmd.119.087809.

101. Saha, G.B. *Physics and Radiobiology of Nuclear Medicine*, 4. Aufl. ed.; Springer-Verlag: New York, NY, 2013.

102. Chomet, M.; van Dongen, G.; Vugts, D.J. State of the Art in Radiolabeling of Antibodies with Common and Uncommon Radiometals for Preclinical and Clinical Immuno-PET. *Bioconjug Chem* 2021, *32*, 1315-1330, doi:10.1021/acs.bioconjchem.1c00136.

103. Bensch, F.; van der Veen, E.L.; Lub-de Hooge, M.N.; Jorritsma-Smit, A.; Boellaard, R.; Kok, I.C.; Oosting, S.F.; Schröder, C.P.; Hiltermann, T.J.N.; van der Wekken, A.J.; et al. ^{89}Zr-atezolizumab imaging as a non-invasive approach to assess clinical response to PD-L1 blockade in cancer. *Nat Med* 2018, *24*, 1852-1858, doi:10.1038/s41591-018-0255-8.

104. Chang, A.J.; Desilva, R.; Jain, S.; Lears, K.; Rogers, B.; Lapi, S. ^{89}Zr-Radiolabeled Trastuzumab Imaging in Orthotopic and Metastatic Breast Tumors. *Pharmaceuticals (Basel)* 2012, *5*, 79-93, doi:10.3390/ph5010079.

105. Velikyan, I.; Schweighofer, P.; Feldwisch, J.; Seemann, J.; Frejd, F.Y.; Lindman, H.; Sorensen, J. Diagnostic HER2-binding radiopharmaceutical, [^{68}Ga]Ga-ABY-025, for routine clinical use in breast cancer patients. *Am J Nucl Med Mol Imaging* 2019, *9*, 12-23.

106. Lofblom, J.; Feldwisch, J.; Tolmachev, V.; Carlsson, J.; Stahl, S.; Frejd, F.Y. Affibody molecules: engineered proteins for therapeutic, diagnostic and biotechnological applications. *FEBS Lett* 2010, *584*, 2670-2680, doi:10.1016/j.febslet.2010.04.014.

107. Orlova, A.; Magnusson, M.; Eriksson, T.L.; Nilsson, M.; Larsson, B.; Höidén-Guthenberg, I.; Widström, C.; Carlsson, J.; Tolmachev, V.; Ståhl, S.; et al. Tumor

imaging using a picomolar affinity HER2 binding affibody molecule. *Cancer Res* 2006, *66*, 4339-4348, doi:10.1158/0008-5472.Can-05-3521.

108. Tolmachev, V.; Orlova, A. Affibody Molecules as Targeting Vectors for PET Imaging. *Cancers (Basel)* 2020, *12*, doi:10.3390/cancers12030651.

109. Hofmann, M.; Maecke, H.; Börner, R.; Weckesser, E.; Schöffski, P.; Oei, L.; Schumacher, J.; Henze, M.; Heppeler, A.; Meyer, J.; et al. Biokinetics and imaging with the somatostatin receptor PET radioligand ^{68}Ga-DOTATOC: preliminary data. *Eur J Nucl Med* 2001, *28*, 1751-1757, doi:10.1007/s002590100639.

110. Farolfi, A.; Calderoni, L.; Mattana, F.; Mei, R.; Telo, S.; Fanti, S.; Castellucci, P. Current and Emerging Clinical Applications of PSMA PET Diagnostic Imaging for Prostate Cancer. *J Nucl Med* 2021, *62*, 596-604, doi:10.2967/jnumed.120.257238.

111. Faviana, P.; Boldrini, L.; Erba, P.A.; Di Stefano, I.; Manassero, F.; Bartoletti, R.; Galli, L.; Gentile, C.; Bardi, M. Gastrin-Releasing Peptide Receptor in Low Grade Prostate Cancer: Can It Be a Better Predictor Than Prostate-Specific Membrane Antigen? *Front Oncol* 2021, *11*, 650249, doi:10.3389/fonc.2021.650249.

112. Varasteh, Z.; Mitran, B.; Rosenstrom, U.; Velikyan, I.; Rosestedt, M.; Lindeberg, G.; Sorensen, J.; Larhed, M.; Tolmachev, V.; Orlova, A. The effect of macrocyclic chelators on the targeting properties of the ^{68}Ga-labeled gastrin releasing peptide receptor antagonist PEG2-RM26. *Nucl Med Biol* 2015, *42*, 446-454, doi:10.1016/j.nucmedbio.2014.12.009.

113. Jansen, K.; Heirbaut, L.; Cheng, J.D.; Joossens, J.; Ryabtsova, O.; Cos, P.; Maes, L.; Lambeir, A.M.; De Meester, I.; Augustyns, K.; et al. Selective Inhibitors of Fibroblast Activation Protein (FAP) with a (4-Quinolinoyl)-glycyl-2-cyanopyrrolidine Scaffold. *ACS Med Chem Lett* 2013, *4*, 491-496, doi:10.1021/ml300410d.

114. Lindner, T.; Loktev, A.; Giesel, F.; Kratochwil, C.; Altmann, A.; Haberkorn, U. Targeting of activated fibroblasts for imaging and therapy. *EJNMMI Radiopharm Chem* 2019, *4*, 16, doi:10.1186/s41181-019-0069-0.

115. Giesel, F.; Adeberg, S.; Syed, M.; Lindner, T.; Jimenez, L.D.; Mavriopoulou, E.; Staudinger, F.; Tonndorf-Martini, E.; Regnery, S.; Rieken, S.; et al. FAPI-74 PET/CT Using Either ^{18}F-AlF or Cold-kit ^{68}Ga-labeling: Biodistribution, Radiation Dosimetry and Tumor Delineation in Lung Cancer Patients. *J Nucl Med* 2020, doi:10.2967/jnumed.120.245084.

116. Ehlerding, E.B.; Ferreira, C.A.; Aluicio-Sarduy, E.; Jiang, D.; Lee, H.J.; Theuer, C.P.; Engle, J.W.; Cai, W. $^{86/90}$Y-Based Theranostics Targeting Angiogenesis in a Murine Breast Cancer Model. *Mol Pharm* 2018, *15*, 2606-2613, doi:10.1021/acs.molpharmaceut.8b00133.

117. Chicheportiche, A.; Ben-Haim, S.; Grozinsky-Glasberg, S.; Oleinikov, K.; Meirovitz, A.; Gross, D.J.; Godefroy, J. Dosimetry after peptide receptor radionuclide therapy: impact of reduced number of post-treatment studies on absorbed dose calculation and on patient management. *EJNMMI Phys* 2020, *7*, 5, doi:10.1186/s40658-020-0273-8.

118. Barca, C.; Griessinger, C.M.; Faust, A.; Depke, D.; Essler, M.; Windhorst, A.D.; Devoogdt, N.; Brindle, K.M.; Schäfers, M.; Zinnhardt, B.; et al. Expanding Theranostic Radiopharmaceuticals for Tumor Diagnosis and Therapy. *Pharmaceuticals (Basel)* 2021, *15*, doi:10.3390/ph15010013.

119. Liu, F.; Zhu, H.; Yu, J.; Han, X.; Xie, Q.; Liu, T.; Xia, C.; Li, N.; Yang, Z. ^{68}Ga/^{177}Lu-labeled DOTA-TATE shows similar imaging and biodistribution in neuroendocrine tumor model. *Tumour Biol* 2017, *39*, 1010428317705519, doi:10.1177/1010428317705519.

120. Nelson, B.J.B.; Andersson, J.D.; Wuest, F. Targeted Alpha Therapy: Progress in Radionuclide Production, Radiochemistry, and Applications. *Pharmaceutics* 2020, *13*, doi:10.3390/pharmaceutics13010049.

121. Kim, E.M.; Jeong, H.J.; Lim, S.T.; Sohn, M.H. Analysis of Cell Fraction of ^{99m}Tc-HMPAO Radiolabeled Leukocytes. *Curr Radiopharm* 2020, *13*, 142-148, doi:10.2174/1874471013666200510015742.

122. Roca, M.; de Vries, E.F.; Jamar, F.; Israel, O.; Signore, A. Guidelines for the labelling of leucocytes with ^{111}In-oxine. Inflammation/Infection Taskgroup of the European Association of Nuclear Medicine. *Eur J Nucl Med Mol Imaging* 2010, *37*, 835-841, doi:10.1007/s00259-010-1393-5.

123. Sammartano, A.; Scarlattei, M.; Migliari, S.; Baldari, G.; Ruffini, L. Validation of in vitro labeling method for human use of heat-damage red blood cells to detect splenic tissue and hemocateretic function. *Acta Biomed* 2019, *90*, 275-280, doi:10.23750/abm.v90i3.7767.

124. Srivastava, S.C.; Chervu, L.R. Radionuclide-labeled red blood cells: current status and future prospects. *Semin Nucl Med* 1984, *14*, 68-82, doi:10.1016/s0001-2998(84)80022-7.

125. Patrick, S.T.; Glowniak, J.V.; Turner, F.E.; Robbins, M.S.; Wolfangel, R.G. Comparison of in vitro RBC labeling with the UltraTag RBC kit versus in vivo labeling. *J Nucl Med* 1991, *32*, 242-244.

126. Currie, G.M.; Towers, P.A.; Wheat, J.M. A role for subtraction scintigraphy in the evaluation of lower gastrointestinal bleeding in the athlete. *Sports Med* 2007, *37*, 923-928, doi:10.2165/00007256-200737100-00007.

127. Dam, H.Q.; Brandon, D.C.; Grantham, V.V.; Hilson, A.J.; Howarth, D.M.; Maurer, A.H.; Stabin, M.G.; Tulchinsky, M.; Ziessman, H.A.; Zuckier, L.S. The SNMMI procedure standard/EANM practice guideline for gastrointestinal bleeding scintigraphy 2.0. *J Nucl Med Technol* 2014, *42*, 308-317, doi:10.2967/jnmt.114.147959.

128. Taefehshokr, N.; Baradaran, B.; Baghbanzadeh, A.; Taefehshokr, S. Promising approaches in cancer immunotherapy. *Immunobiology* 2020, *225*, 151875, doi:10.1016/j.imbio.2019.11.010.

129. Lee, H.W.; Gangadaran, P.; Kalimuthu, S.; Ahn, B.C. Advances in Molecular Imaging Strategies for In Vivo Tracking of Immune Cells. *Biomed Res Int* 2016, *2016*, 1946585, doi:10.1155/2016/1946585.

130. Wolfs, E.; Verfaillie, C.M.; Van Laere, K.; Deroose, C.M. Radiolabeling strategies for radionuclide imaging of stem cells. *Stem Cell Rev Rep* 2015, *11*, 254-274, doi:10.1007/s12015-014-9575-3.

131. de Vries, E.F.; Roca, M.; Jamar, F.; Israel, O.; Signore, A. Guidelines for the labelling of leucocytes with ^{99m}Tc-HMPAO. Inflammation/Infection Taskgroup of the European Association of Nuclear Medicine. *Eur J Nucl Med Mol Imaging* 2010, *37*, 842-848, doi:10.1007/s00259-010-1394-4.

132. Socan, A.; Petrik, M.; Kolenc Peitl, P.; Kroselj, M.; Rangger, C.; Novy, Z.; Svajger, U.; Gmeiner, T.; Decristoforo, C. On-cartridge preparation and evaluation of ^{68}Ga-, ^{89}Zr- and ^{64}Cu-precursors for cell radiolabelling. *Nucl Med Biol* 2019, *71*, 23-31, doi:10.1016/j.nucmedbio.2019.04.001.

133. Freesmeyer, M.; Grober, S.; Greiser, J.; Seifert, P.; Guhne, F.; Drescher, R. PET/CT with [^{68}Ga]gallium-oxine-labeled heat-denatured red blood cells for detection of dystopic splenic tissue. *Eur J Nucl Med Mol Imaging* 2021, *48*, 644-646, doi:10.1007/s00259-020-04899-4.

134. Teiler, J.; Ahl, M.; Åkerlund, B.; Brismar, H.; Holstensson, M.; Gabrielson, S.; Hedlund, H.; Axelsson, R. ^{99m}Tc-HMPAO-WBC SPECT/CT versus ^{18}F-FDG-WBC PET/CT in chronic prosthetic joint infection: a pilot study. *Nucl Med Commun* 2021, doi:10.1097/mnm.0000000000001502.

135. Lim, M.M.D.; Gnerre, J.; Gerard, P. Mechanisms of Uptake of Common Radiopharmaceuticals RadioGraphics Fundamentals Online Presentation. *Radiographics* 2018, *38*, 1550-1551, doi:10.1148/rg.2018180072.

136. Shalaby, N.; Dubois, V.P.; Ronald, J. Molecular imaging of cellular immunotherapies in experimental and therapeutic settings. *Cancer Immunol Immunother* 2021, doi:10.1007/s00262-021-03073-5.

137. Shaikh, F.A.; Kurtys, E.; Kubassova, O.; Roettger, D. Reporter gene imaging and its role in imaging-based drug development. *Drug Discov Today* 2020, *25*, 582-592, doi:10.1016/j.drudis.2019.12.010.

138. Lever, S.Z.; Fan, K.-H.; Lever, J.R. Tactics for preclinical validation of receptor-binding radiotracers. *Nuclear medicine and biology* 2017, *44*, 4-30, doi:10.1016/j.nucmedbio.2016.08.015.

139. Alhajj, M.; Farhana, A. Enzyme Linked Immunosorbent Assay. In *StatPearls*; StatPearls Publishing, Copyright © 2022, StatPearls Publishing LLC.: Treasure Island (FL), 2022.

140. Doctor, A.; Seifert, V.; Ullrich, M.; Hauser, S.; Pietzsch, J. Three-Dimensional Cell Culture Systems in Radiopharmaceutical Cancer Research. *Cancers (Basel)* 2020, *12*, doi:10.3390/cancers12102765.

141. Yee, N.S.; Ignatenko, N.; Finnberg, N.; Lee, N.; Stairs, D. ANIMAL MODELS OF CANCER BIOLOGY. *Cancer growth and metastasis* 2015, *8*, 115-118, doi:10.4137/CGM.S37907.

142. Flecknell, P. Replacement, reduction and refinement. *Altex* 2002, *19*, 73-78.

143. Gillings, N.; Hjelstuen, O.; Ballinger, J.; Behe, M.; Decristoforo, C.; Elsinga, P.; Ferrari, V.; Peitl, P.K.; Koziorowski, J.; Laverman, P.; et al. Guideline on current good radiopharmacy practice (cGRPP) for the small-scale preparation of radiopharmaceuticals. *EJNMMI Radiopharm Chem* 2021, *6*, 8, doi:10.1186/s41181-021-00123-2.

144. Kolenc Peitl, P.; Rangger, C.; Garnuszek, P.; Mikolajczak, R.; Hubalewska-Dydejczyk, A.; Maina, T.; Erba, P.; Decristoforo, C. Clinical translation of theranostic radiopharmaceuticals: Current regulatory status and recent examples. *J Labelled Comp Radiopharm* 2019, *62*, 673-683, doi:10.1002/jlcr.3712.

145. Bormans, G.; Buck, A.; Chiti, A.; Cooper, M.; Croasdale, J.; Desruet, M.; Kumar, V.; Liu, Y.; Penuelas, I.; Rossetti, C.; et al. Position statement on radiopharmaceutical

production for clinical trials. *EJNMMI Radiopharm Chem* 2017, *2*, 12, doi:10.1186/s41181-017-0031-y.

146. Velikyan, I.; Beyer, G.J.; Langstrom, B. Microwave-supported preparation of Ga-68 bioconjugates with high specific radioactivity. *Bioconjugate Chemistry* 2004, *15*, 554-560, doi:DOI 10.1021/bc030078f.

147. Mueller, D.; Klette, I.; Baum, R.P.; Gottschaldt, M.; Schutz, M.K.; Breeman, W.A.P. Simplified NaCl Based Ga-68 Concentration and Labeling Procedure for Rapid Synthesis of Ga-68 Radiopharmaceuticals in High Radiochemical Purity. *Bioconjugate Chemistry* 2012, *23*, 1712-1717, doi:10.1021/bc300103t.

148. Breeman, W.A.P.; de Jong, M.; de Blois, E.; Bernard, B.F.; Konijnenberg, M.; Krenning, E.P. Radiolabelling DOTA-peptides with Ga-68. *European Journal of Nuclear Medicine and Molecular Imaging* 2005, *32*, 478-485, doi:10.1007/s00259-004-1702-y.

149. Arnberg, F.; Lundberg, J.; Soderman, M.; Damberg, P.; Holmin, S. Image-Guided Method in the Rat for Inducing Cortical or Striatal Infarction and for Controlling Cerebral Blood Flow Under MRI. *Stroke* 2012, *43*, 2437-2443, doi:10.1161/Strokeaha.112.655126.

150. Charoenphun, P.; Meszaros, L.K.; Chuamsaamarkkee, K.; Sharif-Paghaleh, E.; Ballinger, J.R.; Ferris, T.J.; Went, M.J.; Mullen, G.E.; Blower, P.J. [^{89}Zr]oxinate$_4$ for long-term in vivo cell tracking by positron emission tomography. *Eur J Nucl Med Mol Imaging* 2015, *42*, 278-287, doi:10.1007/s00259-014-2945-x.

151. Pharmacopoeia, E. Gallium (^{68}Ga) chloride (accelerator-produced) solution for radiolabelling Monograph PA/PH/Exp. 14/T (18) 13 ANP: 3109. 2020.

152. Thisgaard, H.; Kumlin, J.; Langkjaer, N.; Chua, J.; Hook, B.; Jensen, M.; Kassaian, A.; Zeisler, S.; Borjian, S.; Cross, M.; et al. Multi-curie production of gallium-68 on a biomedical cyclotron and automated radiolabelling of PSMA-11 and DOTATATE. *EJNMMI Radiopharm Chem* 2021, *6*, 1, doi:10.1186/s41181-020-00114-9.

153. Pharmacopoeia, E. Gallium (^{68}Ga) edotreotide injection PA/PH/Exp. 14/T (07) 12 COM ANP: 2482. 2011.

154. Clarke, E.T.; Martell, A.E. Stabilities of trivalent metal ion complexes of the tetraacetate derivatives of 12-, 13- and 14-membered tetraazamacrocycles. *Inorganica Chimica Acta* 1991, *190*, 37-46, doi:https://doi.org/10.1016/S0020-1693(00)80229-7.